

12-2010

# Adsorption Isotherms of Diamond-Packed Columns in Reverse Phase Liquid Chromatography

Abraham Kwame Badu-Tawiah  
*Indiana University of Pennsylvania*

Follow this and additional works at: <http://knowledge.library.iup.edu/etd>

---

## Recommended Citation

Badu-Tawiah, Abraham Kwame, "Adsorption Isotherms of Diamond-Packed Columns in Reverse Phase Liquid Chromatography" (2010). *Theses and Dissertations (All)*. 1008.  
<http://knowledge.library.iup.edu/etd/1008>

This Thesis is brought to you for free and open access by Knowledge Repository @ IUP. It has been accepted for inclusion in Theses and Dissertations (All) by an authorized administrator of Knowledge Repository @ IUP. For more information, please contact [cclouser@iup.edu](mailto:cclouser@iup.edu), [sara.parme@iup.edu](mailto:sara.parme@iup.edu).

ADSORPTION ISOTHERMS OF DIAMOND-PACKED COLUMNS IN REVERSE  
PHASE LIQUID CHROMATOGRAPHY

A Thesis

Submitted to the School of Graduate Studies and Research

in Partial Fulfillment of the

Requirements for the Degree

Master of Science

Abraham Kwame Badu-Tawiah

Indiana University of Pennsylvania

December, 2010

Indiana University of Pennsylvania  
The School of Graduate Studies and Research  
Department of Chemistry

We hereby approve the thesis of

Abraham Kwame Badu-Tawiah

Candidate for the degree of Master of Science

---

John C. Ford, Ph.D.  
Associate Professor of Chemistry, Advisor

---

Keith Kyler, Ph.D.  
Associate Professor of Chemistry

---

Jeaju Ko, Ph.D.  
Associate Professor of Chemistry

---

Lawrence Kupchella, Ph.D.  
Assistant Professor of Chemistry

ACCEPTED

---

Timothy P. Mack, Ph.D.  
Dean  
The School of Graduate Studies and Research

Title: Adsorption Isotherms of Diamond-Packed Columns in Reverse Phase Liquid Chromatography

Author: Abraham Kwame Badu-Tawiah

Thesis Chair: Dr. John C. Ford

Thesis Committee members: Dr. Keith Kyler  
Dr. Jeaju Ko  
Dr. Lawrence Kupchella

Adsorption isotherm is a term used to describe relationship between the solute concentration adsorbed onto solid surface and concentration in the mobile phase. In this thesis, attempts were made to measure reliable adsorption isotherms of diamond-packed column in order to study the surface properties of diamond particle. The diamond-packed column was first characterized by measuring the effective particle size, hold-up volume and efficiency of the column using reverse phase liquid chromatography. The measurement of the hold-up volume indicated that the column was well packed. Efficiency of the column was found to agree generally with previous works on diamonds, but showed marked variation for retained compounds. This was attributed to surface defects and it has been recommended that ways must be devised to prevent site defects when packing columns of high density.

Both retention and isotherm results confirm the presence of ionizable groups at the surface of diamond particles produced by chemical vapor deposition as reported by other researchers. Adsorption of acetone on diamond was found to be sensitive to temperature, with similar enthalpy change as those on activated carbon. - The process is exothermic on both adsorbents and low temperature adsorption on diamond appeared to be Langmuirian.

## ACKNOWLEDGEMENTS

I would like to thank my advisor, Dr. John Ford for the time, energy and all the directions he gave me while I was doing the research. To my wife, parents, siblings and friends I say thank you for the support and prayers.

## TABLE OF CONTENTS

Chapter		Page
One	INTRODUCTION.....	1
	Problem Statement.....	4
	Aim.....	4
Two	REVIEW OF RELEVANT LITERATURE.....	5
	Introduction to High Performance Liquid Chromatography.....	5
	Reversed-Phase Liquid Chromatography.....	6
	The Stationary Phase.....	6
	The Mobile Phase.....	7
	Mechanism of RPLC and van't Hoff Plot.....	8
	Efficiency of an HPLC System .....	12
	Column Efficiency.....	12
	Contributions to Band Broadening.....	13
	Efficiency Equations for Modeling Band Broadening.....	14
	Efficiency Calculations.....	18
	Void Volume Determination in Reversed-Phase Liquid Chromatography.....	19
	Methods of Void Volume Measurement.....	20
	Experimental Factors Affecting $V_m$ Measurement.....	24
	Adsorption Isotherm.....	27
	Models of Adsorption Behavior.....	27

## Models of Single-Component Equilibrium

Isotherms.....	27
Type 1: Ideal adsorption on homogeneous surfaces.....	27
The Langmuir Isotherm.....	27
Type 2: Ideal adsorption on heterogeneous surfaces.....	28
The Bi-Langmuir Isotherm.....	29
The Toth Isotherm.....	30
The Fowler Isotherm.....	30
The Freundlich Isotherm.....	31
Type 3: Nonideal adsorption on homogenous surfaces.....	31
The Quadratic Isotherm.....	32
Type 4: Nonideal adsorption on heterogeneous surfaces.....	32
The Martire Isotherm.....	32
Models of Competitive Equilibrium Isotherms.....	34
The Competitive Langmuir Isotherm.....	34
The Competitive Bi-Langmuir Isotherm.....	35

	Methods of Isotherm Measurement.....	35
	Diamond.....	38
	Crystalline Surface Types.....	39
	The (100) surface.....	40
	The (110) surface.....	42
	The (111) surface.....	43
	Diamond's Surface.....	45
Three	EXPERIMENTAL PROCEDURE.....	47
	Materials.....	47
	Equipment and Instrumentation.....	47
	Procedure.....	48
	Isotherm Measurement.....	48
	Thermodynamic Parameter.....	48
Four	RESULTS AND DISCUSSION.....	49
	Void Volume.....	51
	Column Efficiency.....	55
	Adsorption Isotherm.....	56
Five	CONCLUSIONS.....	66
	References.....	67

## LIST OF TABLES

Table		Page
1	Particle size as obtained from different solvents.....	50
2	Void volume of diamond packed column as measured with different solutes in 50% methanol in water, with and without H <sub>3</sub> PO <sub>4</sub> , and with different amounts of KCl .....	52
3	Efficiency of diamond packed column according to solute .....	55

## LIST OF FIGURES

Figure		Page
1	Contributions of A, B and C-term to $H_{tot}$ .....	15
2	Interstitial mobile phase contributions to plate height, as described by the Giddings equation .....	17
3	Self-sharpening boundary in frontal analysis.....	36
4	Illustration of the diffuse rear boundary used in frontal analysis by characteristic point (FACP) measurements.....	36
5	Directions in a crystal .....	40
6	Definition of the index for a plane.....	40
7	Effective particle size versus a property of solvent used.....	51
8	Adsorption data for acetone without fit to any isotherm.....	57
9	Low concentration part of Fig.8 with linear trend.....	58
10	Fit of experimental data to Langmuir Isotherm.....	59
11	Fit of experimental data to quadratic isotherm model.....	63
12	Fit of experimental data to Bi-Langmuir Isotherm model.....	63
13	Example of two plateaus seen in adsorption isotherms of diamond.....	65

## CHAPTER ONE

### INTRODUCTION

Adsorption isotherms have attracted greater attention in recent years as a fundamental tool for investigation of the physical processes involved in chromatographic retention. The key role of the isotherm in analysis and design of preparative- or production-scale chromatographic separations has also contributed to the increasing popularity of this topic [1]. The adsorption isotherm describes quantitatively the equilibrium distribution of a solute between the two phases involved in the chromatographic process over a wide concentration range. Thus, the adsorption isotherm contains information about the solvent, solute, and adsorbent as well as the interactions among these species occurring during adsorption.

Isotherms have been measured traditionally by a static method, in which the change in concentration of a solute upon addition of the adsorbent to the solution is measured and discrete points on the isotherm are calculated from this measurement. The major drawbacks of this technique are the slowness and uncertainty in reaching equilibrium and the large amount of solute required for accurate measurements. Non-polar adsorbents used in reverse-phase chromatography suffer from the additional difficulty that they are poorly wetted by water-rich solvent and this further exacerbates experimental problems.

Chromatographic methods of isotherm measurement have been developed in order to circumvent these problems. The two principal chromatographic methods involve changing the concentration of the solute at the column inlet in a stepwise fashion either up or down. When the concentration is increased, the step develops into a sharp front at

the column outlet while when it is decreased; it becomes a tailing boundary at the outlet. The different shapes of the front and rear are manifestations of the self-sharpening nature of the former (when concentration is changed in a step-up fashion) and the diffuse behavior of the latter (when concentration is changed in a step-down fashion). DeVault [2] pointed out that concave isotherms always exhibit this profile, where the front is sharpened and the back is diffused, but for ideal chromatography without band-spreading the front boundary maintains a square shape as it progresses through the column.

The method that employs the front boundary is termed frontal analysis (FA) and by application of a mass balance provides the surface concentration,  $q(c)$ , in equilibrium with the solute concentration,  $c$ . Thus, one experiment yields one point on the isotherm. The second method, frontal analysis by characteristic point (FACP), calculates the entire isotherm from the concentration profile of the rear boundary. A method related to FACP employs the rear boundary of an overloaded peak, and is called elution by characteristic point (ECP). On the basis of accuracy, precision and speed, De Jong et al [3] (utilizing reverse-phase HPLC) found FA to be the best method. Conder and Purnell [4] and Huber and Gerritse [5, 6], however, measured isotherms by using gas chromatography and preferred FACP and ECP as fast efficient methods, provided non-ideal and kinetic effects were minimized.

Adsorption behavior on silica-bonded hydrocarbonaceous adsorbents used in liquid chromatography was investigated by frontal chromatography (FA and FACP) and elution on a plateau by Horvath *et al* [7]. The relative merits of the various methods of isotherm measurement were compared and it was found that the FA technique was more accurate

and convenient than other methods. Based on these reports, FA was employed in this experiment.

Diamond is one of the two best known allotropes of carbon, whose hardness and high dispersion of light makes it useful for industrial applications and jewelery. Diamond is a transparent crystal of tetrahedrally bonded carbon atoms. Synthetic diamonds were first produced on February 16, 1953 in Stockholm, Sweden by the QUINTUS project of ASEA (*Allmänna Svenska Elektriska Aktiebolaget*). Among the several synthetic methods, chemical vapor deposition (CVD) of diamond has received a great deal of attention in materials science because it allows many new applications of diamond that had previously been either too expensive to implement or too difficult to make economical. CVD diamond growth typically occurs under low pressure (10-200 torr) and involves feeding varying amounts of gasses into a chamber, energizing them and providing conditions for diamond growth on the substrate. Polycrystalline diamond consisting of grain sizes from several nanometers to several micrometers can be grown [8, 9].

Diamond particles have the potential to become a new stationary phase for liquid chromatography. Due to its chemical inertness, this new stationary phase can be applied in a wider pH range than silica particles, which becomes unstable under basic conditions. Telepchak was the first to perform reverse phase adsorption on natural diamond in 1973 [10]. He noted that retention on diamond behaved similarly to that on the inert bonded hydrocarbon phases routinely used in liquid chromatography. In his work, he reported the height equivalent of theoretical plates (HETP) of his column to be 0.66 mm. Nuamthanon in 2002 reported that diamond packed columns have superior selectivity for

polar organic isomers compared with a commonly used silica-based packing material [11].

### Problem Statement

Diamonds have been identified as potentially having especially biocompatible characteristics – cell integrity does not deplete when cultured on diamond surface. Additionally, the process of chemical deposition (coating surfaces with diamonds) has increased in popularity, as of late. However, studies on the surface chemistry of diamonds have been limited to date. Adsorption studies are undoubtedly ways of testing the effectiveness of synthesized diamonds. By better understanding the surface properties of diamonds, we hope that the progress in the field can be expanded and accelerated.

### Aim

The aim of the research is to measure more reliable isotherms on diamond as a function of temperature and determine enthalpy change ( $\Delta H$ ) associated with the process.

## CHAPTER TWO

### REVIEW OF RELEVANT LITERATURE

#### Introduction to High Performance Liquid Chromatography

The Russian botanist Mikhail Tswett was the first to use column packed with calcium carbonate to separate green leaf pigments in 1903 [12]. The bands he observed were colored (*chroma-*), and thus he termed the technique chromatography, which was from the Greek word for “color writing”. Great advancement in the world of chromatography were achieved in the early 1940’s when Martin and Synge published their Nobel Prize winning work on partition chromatography, which employed silica gel as a solid support [12]. The science of liquid chromatography has since come a long way and at present includes a wide variety of separation mechanisms, including those based on adsorption in either normal or reversed-phase mode, ion exchange, and size exclusion. What is common among these apparently different techniques is that they all utilize a liquid mobile phase and separate based on interactions of the sample components with a solid phase.

In the early 1970’s the use of smaller particle sizes and higher pressure limits elevated adsorption chromatography to a new level. This technique was termed High Performance Liquid Chromatography (HPLC) and has, for the last thirty years, been the technique of choice for the separation of complex liquid mixtures. Due to this, HPLC is now a vital tool in many analytical laboratories. The successful separation of such mixtures as human blood, urine, and toxic waste waters have made HPLC indispensable to biomedical research and environmental testing laboratories. Not only is HPLC

regularly used for these purposes, but it has also found permanent use in pharmaceutical labs for the isolation of compounds of interest to drug research.

### Reversed-Phase Liquid Chromatography

The most widely used separation mechanism for liquid chromatography is reversed-phase liquid chromatography (RPLC). Separation in RPLC depends on the hydrophobicity of a solute, which determines the degree of physical interaction of the solute with the stationary phase. The phrase “reversed-phase” is used in reference to the original form of adsorption chromatography known as normal phase liquid chromatography (NPLC) in which a polar stationary phase is used to separate solutes in a nonpolar mobile phase. In the early 1970’s it became apparent to separation scientists that more useful separations would be possible if the phase polarities were reversed, and a nonpolar stationary phase and a polar mobile phase were used. The pressurized mobile phase flow and well-packed columns in HPLC led to efficient separations in reasonable run times for the reversed-phase systems. In addition, the ability to separate both ionic and neutral species caused reversed-phase liquid chromatography to quickly become the most popular form of HPLC available.

#### *The Stationary Phase*

In RPLC, the stationary phase plays a critical role in the separation mechanism. The support particles are typically made of porous, spherical silica. To provide the nonpolar stationary phase surface required in RPLC, the silica particles are chemically modified with an organic moiety, typically a long chain alkyl group such as C<sub>18</sub>.

Following derivatization with the C<sub>18</sub> groups, 3-5 μmol/m<sup>2</sup> of silanol groups remain due to steric hindrance. These residual silanol groups are notorious for causing peak tailing for basic solutes. In an effort to minimize the number of residual silanols, a technique known as end-capping is often performed. The silica is first derivatized with the C<sub>18</sub> chains, followed by a second reaction with trimethylsilyl reagents. These trimethylsilyl groups do not experience the same high level of steric hindrance, and therefore at least some, if not all, of the remaining silanols become derivatized with methyl groups. However, efforts have been and continue to be made to find alternate support material such as alumina or zirconia that might offer greater physical stability under extreme experimental conditions. In this thesis, we demonstrate that diamond can be used as a stationary phase in RPLC.

### *The Mobile Phase*

Unlike in gas chromatography where the mobile phase is merely used as a transport mechanism for the solutes through the column, the mobile phase in liquid chromatography actually plays a crucial role in the separation. For RPLC, the mobile phase is typically a binary mixture of water and an organic solvent, such as methanol, acetonitrile, or tetrahydrofuran. The strength of the mobile phase (i.e. the percent organic in water) determines the rate at which retained solutes elute from the column. In addition to the organic/aqueous mixture, current RPLC mobile phases frequently contain other additives such as buffers, ionic strength adjusters, silanol masking agents, etc. [13].

## Mechanism of RPLC and van't Hoff Plot

Many studies have been conducted that examine the retention mechanism in reverse phase liquid chromatography and two main theories have evolved:

### 1. Solvophobic theory

This was first applied to RPLC by Horvath *et al* in 1978 [14, 15]. In this theory it was proposed that retention is primarily related to hydrophobic interactions between the mobile phase and solutes. The role of the stationary phase is minimized by this theory, and retention is thought to occur through an adsorption rather a partitioning process. A two-step retention mechanism was proposed in the solvophobic theory which involves creation of a solute site cavity in the mobile phase and transfer of the solute to or from the cavity. The driving force behind this theory is the free energy change associated with the two-step solute transfer mechanism.

### 2. Partitioning theory

The partitioning model of retention considers the role of the stationary phase in the retention process. Martire and Boehm in 1983 [16] published the first retention model to consider the effect of stationary-phase chain organization. This statistical mechanical model described the stationary phase as a “breathing” surface that could expand or collapse depending on mobile phase composition.

Dill in 1983 [17] published a partitioning model based on mean-field stationary model theory, which described a three-step molecular process by which the solute transfers from the mobile phase to the stationary phase. This three-step process involves creation of a solute-sized cavity in the stationary phase, transfer of the solute from the mobile phase to the stationary phase and closing of the solute-sized cavity in the

stationary phase. In this model, the solute is thought to be fully embedded in the stationary phase chains rather than adsorbed on the surface. By attachment of the alkyl chains to the silica surface configurational restriction are imposed on them. Because of this, Dill describes the stationary phase as an interface that differs from the bulk system since the surface to volume ratio of an interface is high and its properties vary with depth from the surface. The molecular organization of the interface is determined by the length and bonding density of the alkyl chains attached to the silica surface, as well as the solvent which contacts the chains. In addition, the chains will adopt as much disorder as possible with the geometrical and solvent constraints in keeping with second law of thermodynamics [17].

Partitioning in this case implies that the solvent “embeds” in the constrained stationary- phase chains and differs from bulk-phase partitioning only in the nature of the second liquid, the constrained alkyl chains. According to Dill’s partitioning model, retention process is governed by two factors:

- a) The difference in the contact free energy of the solute in the mobile phase and the stationary phase. This prediction has been studied for a large data base of almost 350 sets of experiments, [18] and in agreement with theory it was found that the dependence of retention on the mobile-phase composition can be corrected to binary interaction contact of solutes with solvent.
- b) The second driving force for retention as predicted by Dill concerns the partial ordering of the grafted alkyl chains, leading to entropic expulsion of the solute from the stationary phase at sufficiently high bonding densities. At low alkyl bond densities, the partitioning of solute should increase linearly up to a critical

bonding density of about 2.7  $\mu\text{mol}/\text{m}^2$ . However, above the critical alkyl bonding density configurational constraints become increasingly important and partitioning becomes “entropically expensive”, leading to a decrease in the partitioning of the solutes.

The effect of alkyl chain bonding density on the partitioning of small non-polar solutes has been tested [19], and a maximum in partitioning coefficient was observed at a bonding density of about 3.1  $\mu\text{mol}/\text{m}^2$ , supporting Dill’s theory. In a separate study, the volume necessary to re-equilibrate a reversed-phase stationary phase following gradient elution was determined as a function of  $\text{C}_{18}$  bonding density [18] and a critical bonding density of about 2.9  $\mu\text{mol}/\text{m}^2$  was observed. This indicates that partitioning of the organic modifiers occurs similarly to the partitioning of small solutes and is also a function of stationary-phase bonding density.

Important information about the retention mechanism in RPLC may be gained by studying the temperature dependence of retention. The temperature dependence of retention is given by

$$\ln k = -\frac{\Delta H}{R} \left( \frac{1}{T} \right) + \frac{\Delta S}{R} + \ln \Phi \quad \text{Eqn 2-1}$$

where  $k$  is the retention factor of the solute,  $\Delta H$  is the enthalpy of transfer of the solute from the mobile phase to the stationary phase,  $\Delta S$  is the entropy of transfer of solute from mobile phase to the stationary phase,  $R$  is the gas constant,  $T$  is the temperature, and  $\Phi$  is the phase ratio of the chromatographic column (the volume of the stationary phase divide by the volume of the mobile phase). This expression indicates that a plot of  $\ln(k)$  versus  $1/T$ , called van’t Hoff plot, has a slope of  $-\Delta H/R$  and an intercept of  $\Delta S/R + \ln \Phi$  if  $\Delta H$  is invariant with temperature (i.e. a linear van’t Hoff plot) is obtained. This provides a

convenient way of calculating the thermodynamic constants  $\Delta H$  and  $\Delta S$  for a chromatographic system if the phase ratio is known or can be calculated. These constants are useful in assessing the thermodynamic driving force for retention.

The temperature dependence of retention has been explored [20, 21]. Linear van't Hoff plots have been observed for various monomeric and polymeric commercially available  $C_{18}$  columns over temperature range of about 30 °C using hydro-organic mobile phase [20-22]. In those studies,  $\Delta H$  values were calculated using the slope of the van't Hoff plots, but  $\Delta S$  values were generally not provided due to ambiguity in the calculation of the phase ratio for commercial columns [23]. In one study  $\Delta S$  values were provided, although a detailed conclusion about the retention mechanism in RPLC were not included since "the structural details of the bonded alkyl phase and the silica gel used as base materials of the commercially available packing materials are usually unknown". In another study, the phase ratio of a commercial column was calculated by using models based on information provided by the manufacturer, and both  $\Delta S$  and  $\Delta H$  were determined [21].

Nonlinear van't Hoff plots have been observed for temperature studies of reversed-phase stationary phase [24-27]. Nonlinear van't Hoff behavior may be indicative of a change in the mechanism of retention. Phase transition of stationary phase may cause nonlinear van't Hoff behavior, but morphological changes in the bonded layer do not necessarily change the intrinsic mechanism. Typically, temperature range of 45° or more have been evaluated in the studies showing nonlinear van't Hoff plots.

## Efficiency of an HPLC System

The productivity of any process is dependent upon the successful operation of its constituent parts, thereby leaving the process vulnerable to its most inefficient step. In the case of liquid chromatography (LC), success depends on the reliability and efficiency of each step in the separation process, including solvent delivery, sample injection, migration through connecting tubing, separation into components within the column, and finally detection of the constituent compounds. In the last three decades, the quality of LC systems as a whole has improved dramatically. Modern instruments employ injectors, detectors, connecting tubing, and column fittings specifically designed to minimize solute band mixing and to prevent any unnecessary loss in efficiency.

### *Column Efficiency*

In HPLC, the efficiency of a system is characteristically measured in the number of theoretical plates  $N$  or as the height equivalent to a theoretical plate  $H$ :

$$N = \frac{t_R^2}{\sigma^2} \quad \text{Eqn 2-3}$$

$$H = \frac{L}{N} \quad \text{Eqn 2-4}$$

$t_R$  is the retention time for a solute,  $\sigma^2$  is the variance of a peak in time units, and  $L$  is the length of the column. Because the variance of a peak is a measure of its width,  $N$  can be considered as a measure of how much a given solute band will spread during its time in the column. In order to compare columns with different particle sizes, the reduced plate height  $h$  is often used as an efficiency parameter:

$$h = \frac{H}{d_p} \quad \text{Eqn 2-5}$$

An efficient HPLC column will have 10,000-20,000 plates and a reduced plate height between 2 and 6; actual values been very dependent on the length of the column.

Also important to practicing chromatographers is the resolution of components in the sample. The resolution of two components is based on the retention time  $t_R$  and the width at the peak base  $W_b$  of the 2 solutes, and is calculated according to Equation 2-6.

$$R = \frac{2(t_{R2} - t_{R1})}{(W_{b1} + W_{b2})} \quad \text{Eqn 2-6}$$

The widths of the peaks are obviously influential for their resolution. Wider peaks lead to less resolution and a lower peak capacity for the system. Therefore, in order for the chromatographers to get the high throughput separations they desire that the causes of band broadening must be identified and minimized.

#### *Contributions to Band Broadening*

The broadening of solute bands has traditionally been ascribed to several kinetic processes taking place within the column. These processes include:

- Multiple flow paths available to solutes, also referred to as eddy dispersion
- Molecular diffusion caused by axial concentration gradients within the column
- Slowness of solute equilibration between the stationary phase and mobile phase
- Resistance to mass transfer in stagnant mobile phase

Many investigators have sought a mathematical equation that describes the different sources of band dispersion. Van Deemter et al in 1956 [28] were the first to propose that the individual processes taking place within the column that lead to broadening of a solute band are independent of one another, and therefore the variance contributions associated with each process are additive. Although the idea of independent variances

has remained relatively whole over the last fifty years, the exact mathematical expression describing these broadening phenomena has been a topic of much debate. Several equations have been proposed to model the in-column dispersion, each relying on theoretical derivations and experimental verification.

### *Efficiency Equations for Modeling Band Broadening*

A brief discussion of the most popular and often-used efficiency equations is provided below. The most obvious difference among the various equations is in the interpretation of the mobile phase contributions to band dispersion.

*van Deemter Equation.* Considered to be the original efficiency equation, the van Deemter equation was derived in 1956 to model the band broadening processes in gas chromatography, but has since been applied to a variety of other separation techniques [28]. The original equation had three terms, A, B, and C, which represented the kinetic processes responsible for the spreading of the solute band. Later, the C term was split in two separate terms,  $C_s$  and  $C_m$ . Equation 2-7 is the version of the van Deemter equation most often used today.

$$H = A + Bu + C_m u + C_s u \quad \text{Eqn 2-7}$$

A, B, and C-term contributions to  $H_{\text{tot}}$  as described by the van Deemter equation is shown in Figure 1,  $u$  being the mobile phase velocity.

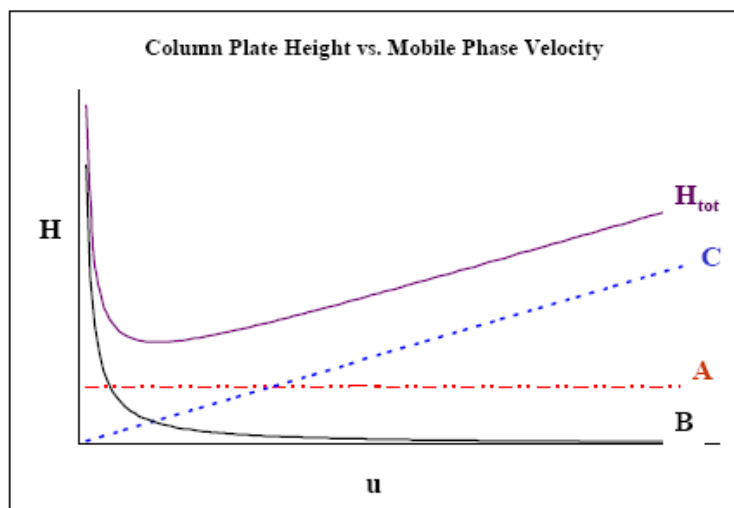


Figure 1: Contributions of A, B and C-term to  $H_{tot}$

A-term describes broadening due to the unequal flow paths available to the solutes in packed columns. B-term describes broadening due to the diffusion of molecules in a sample band as a result of axial concentration gradients. C-term is known as the resistance to mass transfer term and represents a contribution to band dispersion caused by the slow kinetics associated with the transfer of a solute between the mobile and stationary phases.

*Giddings Equation.* J. Calvin Giddings was not satisfied with the van Deemter equation and its depiction of band broadening in the interstitial space of the column [29]. Primarily, Giddings believed the A-term broadening contribution and the  $C_m$ -term did not act independently and therefore did not produce additive variances. Giddings proposed a new idea in an attempt to explain experimental deviations from the van Deemter equation. His theory corresponded to conventional thought concerning the existence of various flow paths available to solutes in a sample band; however he explained it with respect to velocity inequalities rather than distance inequalities.

According to Giddings' theory, in a randomly packed bed the distance and path width between any two particles, which affects the solute velocity, will depend on the packing density of that region. This leads to a radial velocity heterogeneity that results in dispersion of the solute band, which can only be prevented if the solute band samples the entire range of velocities. In both open tubular and packed column chromatography, this is accomplished by radial or lateral diffusion. However, in packed column chromatography, the radial diffusion is aided by the column packing, which forces a solute molecule to leave its current flow path and enter another, thus leading to an attenuation of velocity inequalities. Giddings believed this represented a coupling of effects which determined the amount of spreading in the mobile phase. Rather than directly adding the variances due to flow path inequality and solute transfer in the mobile phase, he claimed their variances should be harmonically combined, because together they actually worked to decrease the amount of spreading. Therefore, the coupled sum of the two terms should theoretically be less than either of the individual contributions, as shown in Figure 2.

The Giddings equation can be mathematically expressed as follows:

$$H = \frac{1}{\frac{1}{A} + \frac{1}{C_m u}} + \frac{B}{u} + Cu \quad \text{Eqn 2-8}$$

The first term in Equation 2-8 is the coupling term of Giddings, which describes the contributions of mobile phase effects taking place within the interstitial moving zone. This term represented an attenuation of band spreading by the cooperative effects of eddy dispersion and transverse diffusion in the mobile phase. At low mobile phase velocities, the  $C_m$  contribution will dominate, leading to a linear increase in plate height. At higher

velocities, the velocity-independent A-term will dominate, resulting in a constant contribution to plate height, as shown in Figure 2. The B-term in the Giddings equation is identical to that in the van Deemter equation, and describes molecular diffusion taking place within the solute band. The C-term strongly resembles the  $C_s$  term of the van Deemter equation, and accounts for all contributions to plate height from the stationary zone, which included resistance to mass transfer of the solute within the stationary phase and any stagnant mobile phase.

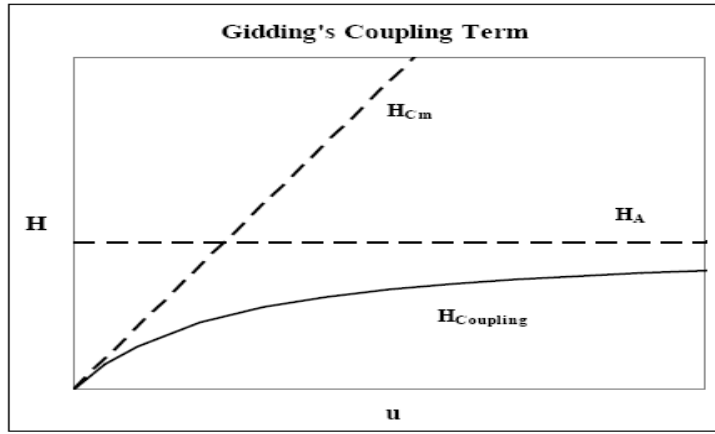


Figure 2. Interstitial mobile phase contributions to plate height, as described by the Giddings equation [29].

Other efficiency equations for modeling band broadening include the *Horvarth & Lin equation* [30], (Eqn 2-9) and the *Knox equation* [31], (Eqn 2-10)

$$H = \frac{1}{\frac{1}{A} + \frac{1}{Cu_e^{1/3}}} + \frac{B}{u_e} + Du_e^{2/3} + Eu_e \quad \text{Eqn 2-9}$$

In Eqn 2-9, the D-term was included to account for the resistance to mass transfer of the solute in the stagnant layer surrounding the particles for solutes with access to support particle interiors and E-term, contribution for a non retained solute, which

described diffusion through the stagnant mobile phase, collected within the particle, and had a linear contribution to plate height.  $u_e$  represented the mobile phase velocity.

Rather than developing a new efficiency equation based on theoretical principles, Knox *et al* proposed an empirical equation to model plate height due to the broadening taking place in the column [31].

$$h = Av^{1/3} + Bv + Cv \quad \text{Eqn 2-10}$$

According to Knox, a well-packed column will have values such as  $A = 1$ ,  $B = 2$ , and  $C = 0.1$  [32].  $v$  is the reduced velocity.

### *Efficiency Calculations*

Accurate calculation of efficiency parameters is critical for the proper interpretation of plate height data.

The number of theoretical plates  $N$  is defined as the ratio of the square of the center of mass of a peak (COM) to the variance of a peak [33].

$$N = \frac{COM^2}{\sigma^2} \quad \text{Eqn 2-11}$$

A large value of  $N$  indicates a small amount of variance, or band spreading, during the time of solute retention within the column. In practical terms,  $N$  is often measured as the ratio of the square of the retention time at the peak maximum for a particular solute to the square of the width of the solute peak.

$$N \approx \frac{t_R^2}{W^2} \quad \text{Eqn 2-12}$$

Controversy arises over what should be considered the true variance of the peak and how it should be related to a measurable width [34]. Assuming a Gaussian peak

shape, equations have been derived which use  $W_b$ , the width at the base of the peak,  $W_i$ , the width at the inflection points of the peak, and  $W_{0.5}$ , the width at 50% of the peak maximum, as shown in Equations 2-13 through 2-15 below.

$$N = 16 \left( \frac{t_R}{W_b} \right)^2 \quad \text{Eqn 2-13}$$

$$N = 4 \left( \frac{t_R}{W_i} \right)^2 \quad \text{Eqn 2-14}$$

$$N = 5.54 \left( \frac{t_R}{W_{0.5}} \right)^2 \quad \text{Eqn 2-15}$$

#### Void Volume Determination in Reversed-Phase Liquid Chromatography

In modern, bonded-phase RPLC, the mobile phase is a liquid, and the stationary phase is at least liquid-like. This complicates the placement of any boundary between them. The silica particles used as the stationary phase support in RPLC are extremely porous, comprising an estimated 30% of the total volume in the column. Within this pore space there is no convective velocity. Therefore, the mobile phase that is being pressure-driven through the column collects in the pores and becomes stagnant. Also, trapped regions of mobile phase exist in the niches between silica particles. These trapped regions of mobile phase are no longer moving, so should they be considered mobile phase? Some authors believe there should be no distinction between the moving and nonmoving regions of mobile phase, due to the complexity of boundary placement between mobile and stationary phases. These authors recommend the measurement of the entire volume of liquid in the column as the void volume ( $V_m$ ) [35-37]. In contrast, there are other researchers who advocate the use of only the moving regions of mobile phase as a

measure of  $V_m$ , choosing not to measure any regions of mobile phase immobilized by the stationary phase [38, 39].

Alhedai *et al.* provided a detailed analysis of the various regions comprising the mobile phase volume in a RPLC column [40]. In their analysis, a distinction was made between the kinetic and the thermodynamic void volumes. The kinetic void volume was comprised of only the moving portion of mobile phase, and was considered to be a constant parameter of the column. This measure of  $V_m$  was recommended for all kinetic measurements, and would be independent of the particular solute chromatographed. The thermodynamic void volume represented all regions of mobile phase, both stagnant and moving, that had the same composition as the bulk phase [40].

A more practical definition of  $V_m$  is the volume of mobile phase required to elute an unretained compound [41]. This is possibly the most commonly used definition of the void volume because of its obvious method of measurement – the injection of an unretained compound. However, the simplicity of this definition belies the actual complexity associated with the measurement. Controversy over this particular definition exists in many areas, including the choice of unretained compound, the possibility of weak retention, and the degree to which the probe compounds are able to explore the regions of stationary phase.

#### *Methods of Void Volume Measurement*

Because researchers have been unable to assign a universal definition to the void volume in RPLC, a standard procedure has also not been developed for its measurement. A brief scan of the literature over the past 30 years shows the diverse array of methods

for measuring such an apparently simple parameter. However, the majority of these can be simplified and categorized into 4 divisions. These include a static method known as pycnometry, chromatographic methods using inorganic salts or neutral organics as unretained markers, a baseline disturbance method, and a mathematical technique that uses the retention time of a series of homologous compounds to calculate the volume of mobile phase in a column.

**Pycnometry.** Pycnometry, also known as the weight difference method, is the most widely recognized non-chromatographic method of  $V_m$  measurement. This technique typically employs two organic solvents with different densities. A chromatographic column is first equilibrated with one solvent, and its mass carefully measured. The column is then equilibrated with the second solvent, followed again by mass measurement. Using the solvent densities,  $\rho_x$  and  $\rho_y$ , and the corresponding column masses,  $W_x$  and  $W_y$ , the void volume of the column is calculated as follows [42]:

$$V_0 = \frac{W_x - W_y}{\rho_x - \rho_y} \quad \text{Eqn 2-16}$$

Commonly used solvents include methanol ( $\rho = 0.7866$  g/mL), acetonitrile ( $\rho = 0.7138$  g/mL), chloroform ( $\rho = 1.484$  g/mL), and carbon tetrachloride ( $\rho = 1.589$  g/mL). The small size of the solvent molecules allows them to access all space within the column, including areas not accessible to some solutes. Pycnometry measures the entire volume of liquid phase within the column, including any solvent molecules found in the stationary phase solvation layer. Therefore, it is generally agreed that  $V_m$  measured pycnometrically gives a maximum value for the void volume, and has been used for this purpose by many workers [40, 42-45]. However, there have been some workers critical of

pycnometry, claiming this measurement overestimates the true void volume of the column [46, 47].

**Unretained compounds.** The simplicity and ease of injecting an unretained compound makes this method the most common method of  $V_m$  measurement. The only requirement for a suitable  $V_m$  marker is that it must have no interaction with the stationary phase, thus no retention. Although not a requirement, a practical criterion for a  $V_m$  marker is that it is able to absorb UV light, and therefore easily detected. The ideal  $V_m$  marker should have access to all space within the column, including pore volume, without being excluded from any space or interacting with the nonpolar stationary phase. Commonly used  $V_m$  markers fall into two categories: neutral organic compounds and inorganic salts. Though these compounds are quite popular for  $V_m$  measurement, it is debatable whether they satisfy the requirements for an ideal marker.

*Neutral Organics.* The neutral organic solutes most often used for  $V_m$  measurement include uracil [48-50], urea [50], thiourea [51, 52], acetone [53, 49, 50], and phloroglucinol [54, 55]. These compounds are all small enough to access the pore volumes in the column and can successfully be used with UV detection. However, it has been shown that the void times of these and similar compounds increased as the mobile phase strength decreased from ~50% organic to pure water [33]. In other words, the solutes spent more time in the column as the percent of organic modifier in the mobile phase was decreased. Under reversed-phase conditions, this would imply retention of the solutes on the column. However, the situation becomes more complicated at organic

modifier compositions above 50%. The measured void volumes go through a minimum before increasing at higher percent organic [47, 56].

It has also been shown that as the temperature was decreased [44, 49], the retention time of the solutes increased. This temperature dependence has been attributed to an expansion of the C<sub>18</sub> chains and an increased mobility of the chains at higher temperatures [44]. The neutral organic compounds are convenient and provide reproducible data, but they should be used with caution as void volume markers.

*Inorganic Salts.* Inorganic salts used as V<sub>m</sub> markers have many similar characteristics to the neutral organics, including convenience, small size, and UV detectability. Commonly used salts include NaNO<sub>3</sub>, NaNO<sub>2</sub>, KI, K<sub>2</sub>Cr<sub>2</sub>O<sub>7</sub>, and KBr. Unlike the neutral organics, inorganic salts do not typically show a significant retention time dependence on either mobile phase composition or temperature, making them more suitable test solutes. However, the salts are not without problems. It has been shown by many workers that the retention time of the salts increases with increasing sample concentration, or amount. This phenomenon has been well-documented, and is referred to as the Donnan effect, or Donnan exclusion [57-59].

**Minor Disturbance.** The minor disturbance method is another popular chromatographic technique for measuring the void volume in RPLC. There are several variations of this method, but all essentially detect a disturbance in the baseline. The most convenient technique for creating a baseline disturbance is to inject a pure sample of a mobile phase component, and use this directly as a measure of the void volume. Theoretically, when a sample is injected that contains mobile phase components not in

the same ratio as the bulk liquid, the equilibrium established for these mobile phase components between the mobile and stationary phase is disturbed. This minor disturbance travels through the column at the same rate as the bulk mobile phase, and its elution time provides a measure of the void volume in the column. Multiple peaks are likely to be seen when pure components are injected. To avoid this, the sample must contain mobile phase with the same composition as the bulk phase; however, a baseline disturbance of this sort would be very difficult to detect. To avoid this issue, many researchers use isotopically labeled mobile phase components, which create a baseline disturbance due to a change in the refractive index of the eluent [56, 60]. This change can be monitored using a refractive index detector or a UV-Vis detector set at low wavelengths.

#### *Experimental Factors Affecting $V_m$ Measurement*

The void volume of a reversed-phase column is obviously a much more complex parameter than many originally thought. Not only is it difficult to define and measure, but the conditions under which it is measured have also been shown to affect its proper assessment. It has been demonstrated by several authors that experimental conditions such as temperature, mobile phase composition, and pH can alter  $V_m$  measurements.

**Temperature.** A decrease in the void volume measured by some neutral organic compounds as the experimental temperature increased has been demonstrated [37, 44, 61]. It was suggested that the source of this was either a decrease in viscosity of the mobile phase, an increase in the diffusion of the compounds, or possibly changes in

retention [44]. Other authors attributed this behavior to thermal expansion of the column hardware, the silica matrix, the bonded phase, or the eluent [37]. It has been postulated that at higher temperatures the stationary phase chains expand and become more mobile, thus decreasing the measured void volume [44]. Therefore, it is imperative for the temperature at which RPLC experiments are conducted remain constant for an accurate measurement of the void volume.

**Mobile Phase Composition.** The mobile phase composition has also been shown to affect  $V_m$  measurements. For neutral organic compounds, changes in retention time were observed when varying mobile phase strength, or the amount of organic modifier [56, 57, and 62]. Studies on the dependence of measured void volume on the mobile phase concentration as determined by salts have also been conducted [59], and it was shown that a change in elution volume was indeed observed, but the change was insignificant compared to injections of neutral organics or mobile phase components.  $V_m$  measured by the homologous series method was monitored over the mobile phase composition [63], as was the injection of mobile phase components [60, 61]. It was postulated that the cause of these effects was related to the conformation of the bonded phase chains. In a highly organic mobile phase, it was believed that the stationary phase chains were extended, thus partially blocking the pores. As the organic content was reduced, the chains collapsed, thus opening the pores for probe molecule entry and increasing the measured void volume [43].

**pH.** For charged compounds, the mobile phase pH has been shown to affect the access probes have to the stationary phase pores [58, 59, and 64]. In particular, inorganic salts are excluded from the pore volume due to the electrostatic repulsion of the residual

silanol groups on the silica surface. Therefore, in order to obtain reproducible results, it is necessary to buffer the mobile phase to a consistent pH.

**Mobile Phase Flow Rate.** In addition to the above mentioned factors, the mobile phase flow rate also influences the chromatographic measurement of void volume. Theoretically, solutes used as unretained markers should not interact with the stationary phase, and therefore, should not be retained. Their mode of transport through the column is the moving mobile phase, but it is their ability to diffuse that allows these compounds to sample the space within the stationary phase pores. If these regions are not fully sampled, the measured void volume will not accurately represent the mobile phase volume. Because these solutes must diffuse into and out of the pores, the extent of their movement is limited by the rate of mobile phase flow. At too high flow rates, the solutes may simply not have enough time to fully sample the regions of the column that the pressure-driven flow does not allow them to easily access. The solvent in the stationary phase pores should have the same composition as the solvent in the bulk flow. Therefore, the probe solutes should not experience an energy barrier when diffusing from interstitial to intraparticle space. However, if the solutes do not have enough time to fully diffuse into the pore space, i.e., if the process is time-limited, the elution volume of the markers will not accurately represent the column void volume.

## Adsorption Isotherm

### *Models of Adsorption Behavior*

Numerous theories have been advanced to describe adsorption, based on assumptions about the solute, the physical process of adsorption and/or the shape of the isotherm [1].

#### *a) Model of Single-Component Equilibrium Isotherms*

There are four types of single-component equilibrium isotherms, for adsorption with or without solute-solute interactions, on homogeneous or heterogeneous surfaces

##### *Type 1: Ideal adsorption on homogeneous surfaces*

The two models of this type are Langmuir [6, 65] and Jovanovic [66]. These models are rarely found in HPLC, except for mildly polar, acidic compounds in normal phase HPLC [5].

##### *The Langmuir Isotherm*

Langmuir [6] proposed an adsorption model in 1916 for adsorption in a gas-solid system. He assumed a constant heat of adsorption and finite number of surface adsorption sites. With these assumptions maximum adsorption corresponds to a saturated monolayer of solute molecules on the adsorbent surface. The Langmuir equation for liquid-solid adsorption is

$$q = \frac{aC}{1+bC} \quad \text{Eqn 2-17}$$

where  $q$  is the amount of solute on one unit of adsorbent,  $C$  is the mobile phase concentration, and  $b$  is an empirical constant related to the energy of adsorption.

Isotherms in reverse-phase liquid chromatography have been found to follow this general behavior up to the point of saturation of the stationary phase. At higher concentrations, however, this is no longer valid [67]. Parameter  $a$  is the isotherm slope at low solute concentration and within this range

$$a = K$$

where  $K$  is the equilibrium constant for the sorption process in the domain of Henry's law and is related to the retention factor,  $k$ , by

$$k = K\Phi$$

where  $\Phi$  represents the phase ratio.

#### *Type 2: Ideal adsorption on heterogeneous surfaces*

Experimental results show that many systems of chromatographic interest follow this type of behavior because:

1. Packing materials for chromatography are carefully prepared adsorbents with a more homogeneous surface than most conventional adsorbents [68].
2. Also, the activity coefficients in solution and in the adsorbed state vary with the concentration, as demonstrated by Carr *et al* [69] and confirmed by calculations [70] based on UNIFAC model [71].

Examples of isotherm models under this type are bi-Langmuir [72], Toth [73], Fowler isotherm and Freundlich isotherm models.

### The Bi-Langmuir Isotherm

In many cases, the surface of the adsorbent used for chromatographic separations is not homogeneous. The simplest model for a non-homogeneous surface is a mixed surface covered with two different kinds of chemical groups, a model which applies well to chemically bonded alkyl silica with a moderate bonding density [1]. Part of the surface is covered by the alkyl groups and is quite hydrophobic, resulting in nonspecific interactions with the retained components. The rest of the surface is covered with siloxane groups (silica), which are Lewis bases, and with silanol groups, which are acid groups. This structure makes the alkyl bonded silica a hydrophilic adsorbent, able to give strong polar interactions with all polar compounds.

With such a surface covered with two different kinds of sites which behave independently, the equilibrium isotherm results from the addition of the two independent contributions of the two sites [74]. Such an isotherm is called a bi-Langmuir isotherm. Since in most cases the Langmuir isotherm is appropriate to account for single-component adsorption on a homogeneous surface, we have the following isotherm:

$$q = \frac{a_1 C}{1 + b_1 C} + \frac{a_2 C}{1 + b_2 C} \quad \text{Eqn 2-18}$$

where the subscript refers to the type of adsorption sites.

The bi-Langmuir isotherm was first suggested by Graham [75] to account for adsorption behavior on certain inhomogeneous surfaces. It has been used successfully by Laub [76] in gas chromatography.

### The Toth Isotherm

The Toth isotherm [77] was originally derived for the study of gas-solid equilibria, however, like the Langmuir isotherm model, it can be extended to the description of liquid-solid system. It assumes a continuous and possibly wide adsorption energy distribution and has a finite Henry constant, hence predicts finite retention time at finite dilution. The equation of the Toth isotherm is:

$$\Theta = \frac{q}{q_s} = \frac{C}{(b + C^t)^{1/t}} \quad \text{Eqn 2-19}$$

This isotherm is similar to the Langmuir model, to which it becomes identical for  $t = 1$ . The parameters  $b$  and  $t$  permit independent adjustment of the initial slope and curvature of the isotherm. This model has been used successfully to account for experimental isotherm data regarding gas-solid adsorption.

### The Fowler Isotherm

The Fowler isotherm was designed by Fowler and Guggenheim [1] to correct for the first-order deviation from the Langmuir isotherm. It assumes ideal adsorption on localized sites with weak interaction between molecules adsorbed on neighboring sites. It also assumes that the interaction energy between two solute molecules is small enough that the random character of the solute molecule distribution on the adsorbent surface is not significantly altered. Under these assumptions, the following gas-solid isotherm is obtained

$$bP = \frac{\Theta}{1 - \Theta} e^{2w\Theta/RT} \quad \text{Eqn 2-20}$$

where  $\Theta$  is the degree of surface covered and  $2w$  is the interaction energy between the molecules in a pair of neighbors;  $P$  is the partial pressure. For liquid-solid equilibria, the Fowler isotherm is extended empirically and written as:

$$bCe^{-X^\Theta} = \frac{\Theta}{1-\Theta} \quad \text{Eqn 2-21}$$

where  $X$  is an empirical interaction energy parameter and  $C$  is the mobile phase concentration.

### The Freundlich Isotherm

The Freundlich isotherm equation is an empirical equation and may be derived by assuming a heterogeneous surface with adsorption on each class of sites that have obeyed the Langmuir equation [77]. According to the Freundlich equation, the amount adsorbed increases infinitely with increasing concentration [78]. This equation is, therefore, satisfactory for low concentration. The Freundlich equation is commonly used as

$$q = K_F C^{1/n} \quad \text{Eqn 2-22}$$

where  $q$  is the adsorption capacity,  $C$  is the adsorption equilibrium concentration and  $K_F$  and  $n$  are empirical constants, which depend on the nature of adsorbent and adsorbate, and on the temperature.

### *Type 3: Nonideal adsorption on homogenous surfaces*

Depending on the extent of solute-solute interactions, the isotherm is convex or S-shaped. Common isotherm models are the quadratic, the extended BET, and the Moreau isotherm. All tend toward the Langmuir model when the solute-solute interactions tend towards zero.

### The Quadratic Isotherm

The equation of the quadratic isotherm is given by:

$$\Theta = \frac{b_1 C + 2b_2 C^2}{1 + b_1 C + b_2 C^2} \quad \text{Eqn 2-23}$$

This isotherm, suggested by simple statistical thermodynamic, is useful to account for isotherms having an inflection point [79]. The curvature of this isotherm at the origin and at low concentrations is concave upwards, which indicate that the amount adsorbed at equilibrium increases more rapidly than the concentration in the mobile phase. Such an effect results from strong solute-solute interactions, e.g., stacking of nucleotides or of large, planar, polycyclic aromatic compounds.

### *Type 4: Nonideal adsorption on heterogeneous surfaces*

Among the many complex models, the best known are the Martire and the bi-Moreau isotherms [4]. High accuracy data are required for reasonably precise estimates of the numerous parameters of the models.

### The Martire Isotherm

This model was developed using statistical thermodynamics and the mean field lattice model. It can be applied as well to gas, liquid, and supercritical chromatography. The isotherm is given by the following equation:

$$\frac{K_i^0 \Theta_{i,m} e^{(D_{i,m} \Theta_{i,m})}}{1 - \Theta_{i,m}} = \frac{\Theta_{i,m} e^{[(1-f_i) D_{i,s} \Theta_{i,s}]}}{(1 - \Theta_{i,s})^{f_i}} \quad \text{Eqn 2-24}$$

where  $f_i$  is the fraction of the total surface area of the solute molecule  $i$  which comes in contact with the adsorbent surface;  $\Theta_{i,m}$  and  $\Theta_{i,s}$  are the volume fractions of the solute in

the mobile phase and stationary phase, respectively;  $\mathbf{U}_i = \mathbf{r}_i/\mathbf{r}_c = \mathbf{U}_i^*/\mathbf{U}_c^*$  with  $\mathbf{r}_i$  and  $\mathbf{r}_c$ , being the numbers of adsorbent sites occupied by the solute and solvent respectively, and  $\mathbf{U}_i$  and  $\mathbf{U}_c$  being the van der Waals molar volumes of the solute and solvent respectively; and  $K_i^0$  is the ratio of the equilibrium concentrations of the solute in the stationary and mobile phases at infinite dilution of the solute:

$$K_{i,0} = \lim(\Theta_{i,m \rightarrow 0}) C_{i,s} / C_{i,m} = \Theta_{i,s} / \Theta_{i,m} \quad \text{Eqn 2-25}$$

and  $D_{i,m}$  is an interaction term given by:

$$D_{i,m} = -2\mathbf{r}_i \chi_{i,c} = \frac{Z_e \mathbf{r}_i}{k_B T} [2\epsilon_{i,c} - (\epsilon_{i,i} + \epsilon_{c,c})] \quad \text{Eqn 2-26}$$

where  $\epsilon_{i,i}$ ,  $\epsilon_{c,c}$  and  $\epsilon_{i,c}$  are the attractive interactive energies between nearest neighbor segments for the solute-solute, solvent-solvent, and solute-solvent molecules, respectively;  $\chi_{i,c}$  is the interactive parameter;  $Z_e$  is the number of nearest neighbors, or external contacts of a molecular segment;  $T$  is the absolute temperature; and  $k_B$  is the Boltzmann constant.

One major feature of this isotherm is its generality. If we assume that the solutions are energetically ideal,  $\chi_{i,c} = D_i = 0$ . Assuming further that  $\mathbf{U}_i = 1$  and that the solution is dilute (i.e.  $\Theta_{i,m} \ll 1$ ) yields the Langmuir isotherm. If only the adsorbed phase is not ideal ( $D_{i,m} = 0$ ,  $D_{i,s} \neq 0$ ) but still assuming that  $\mathbf{U}_i = 1$  and that solution is dilute, ( $\Theta_{i,m} \ll 1$ ), it reduces to the Fowler isotherm.

### *b) Models of Competitive Equilibrium Isotherms*

The study of separation problems requires the use of competitive isotherms. Many single-component models can be extended to competitive isotherms. However, competitive isotherms must be consistent with the Gibbs isotherm equation, given by

$$A(\partial\pi / \partial p) = \frac{RT}{p} n_{ads} \quad \text{Eqn 2-27}$$

where A is the surface area and  $\pi$  is the spreading pressure.

#### *The Competitive Langmuir Isotherm*

The competitive Langmuir isotherm for the  $i^{\text{th}}$  component in the multicomponent system is given by:

$$q_i = \frac{a_i C_i}{1 + \sum_{i=1}^n b_i C_i} \quad \text{Eqn 2-28}$$

where n is the number of components in the system. The coefficients  $a_i$  and  $b_i$  are the coefficients of the single component Langmuir equilibrium isotherm for component i. It seems from the above equation that the competitive Langmuir isotherm is true only if all the components have the same column saturation capacities, a condition not often met, except in the case of enantiomers [80] for which the model gives excellent results. However, it is observed that the separation factor is constant, independent of the relative composition of the mixture. The separation factor for a binary mixture is by the equation:

$$\alpha = \frac{q_2 / C_2}{q_1 / C_1} = \alpha_1 / \alpha_2 \quad \text{Eqn 2-29}$$

As a consequence, the competitive Langmuir isotherm model offers no possibility to account for a reversal in the elution order of two components with increasing

concentration. On the contrary, experimental results show that such an inversion is possible, and that it is not even unusual when the column saturation capacities of the two single-component isotherms are very different.

### *The Competitive Bi-Langmuir Isotherm*

By analogy to the competitive Langmuir isotherm, when a surface is covered with two different kind of sites, we can account for the competitive behavior of two components using a bi-Langmuir isotherm:

$$q_i = \frac{a_{i,1}C_i}{1 + b_{A,1}C_A + b_{B,1}C_B} + \frac{a_{i,2}C_i}{1 + b_{A,2}C_A + b_{B,2}C_B} \quad \text{Eqn 2-30}$$

The coefficients of this competitive isotherm are those obtained for the single-component isotherms of the two components

### Methods of Isotherm Measurement

Glueckauf [81] was the first to use chromatography to measure isotherms as pointed out by Conder and Young [82], who gave a comprehensive review of the methods for gas chromatographic measurement of isotherms. These methods are readily extended to HPLC. The most straightforward chromatographic technique is frontal analysis (FA), introduced by James and Philips [83] and Schay and Szekely [84]. It relates the velocity of the concentration front formed by a step increase in concentration of a solute to the value of the solute's adsorption isotherm at the elevated concentration. Fig. 1 depicts the effluent profile after changing the concentration from  $c_a$  to  $c_b$ , and an integral mass balance shows that the stationary phase concentration of the solute in equilibrium with  $c_b$  is given by

$$q(c_b) = q(c_a) + \frac{(c_b - c_a)(V_F - V_D)}{V_{sp}} \quad \text{Eqn 2-31}$$

where  $q(c_a)$  is the concentration of adsorbed solute in equilibrium with  $c_a$ ,  $V_F$  is the retention volume of the front,  $V_D$  is the system dead-volume, including column hold-up volume, and  $V_{sp}$  is the volume of adsorbent in the column. Repeating this operation with successive higher concentrated solutions yields additional discrete points on the isotherm.

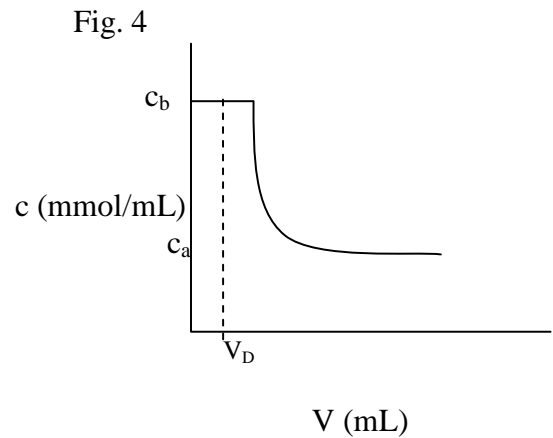
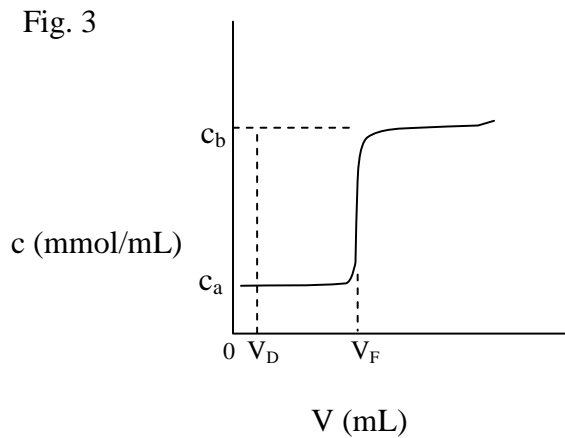


Fig. 3: Self-sharpening boundary in frontal analysis.

Fig. 4: Illustration of the diffuse rear boundary used in frontal analysis by characteristic point (FACP) measurements.

The diffuse rear boundary is employed by the frontal analysis by characteristic point (FACP) method, introduced by Glueckauf [81], and permits construction of the entire isotherm from one experiment, in which the concentration of the solution pumped into the column is changed only once. FACP, in contrast to FA, reconstructs the isotherm from measurements on the diffuse rear boundary that arises from a step decrease in concentration. Such a rear boundary is shown in Fig. 3 as a function of the concentration

profile recorded at the column outlet,  $c(V)$ , where  $V$  is the volume of the effluent. A differential mass balance yields

$$q(c) = 1/V_{sp} \int (V - V_D) dc \quad \text{Eqn 2-32}$$

as the governing equation for determination by FACP. Since the detector signal must be converted into concentration units in order to evaluate  $q(c)$  in the above equation, (Eqn 2-32) calibration of the detector is necessary. Another drawback of FACP is that no correction is made to account for band spreading, which will broaden and diffuse the boundary depicted in Fig. 4. The FA method, since it depends on accurate measurement of the retention time of a self-sharpening front, is less prone to error from this source.

Several methods similar to FACP have appeared that are based on eqn. 2-32 but determine  $V(c)$  in a different manner, including elution by characteristic point (ECP) from Cremer and Huber [85] and elution on a plateau (EP), introduced by Reilley *et al* [86]. ECP is identical to FACP, except a limited amount of solute is injected such that an elution peak results, rather than a decreased in concentration from a plateau. Analysis, using Eqn.2-32 is then carried out on the rear boundary of the peak. The advantage of this technique is the small amount of sample required, but it has the same disadvantage as FACP. In EP the column is equilibrated with a solution at a given concentration, and the retention volume of the perturbation of that concentration is measured to yield  $V(c)$ , which can be treated in manner analogous to  $c(V)$ . Thus no calibration of detector is necessary, and the inaccuracy associated with band spreading for FACP is largely reduced. However, the detection problems with common HPLC equipment at high concentrations can be significant, the size of the perturbation can influence the accuracy

of the result, solute consumption is substantial and the experimental complexity is greater than that for FA technique, all of which argue against EP.

### Diamond

The chemical nature of the surface of the diamond particles used in this investigation is complex: it is probably most structurally similar to the idealized (111) surface, consisting of a mixture of  $sp^3$ - and  $sp^2$ -hybridized carbons and a modestly low density of probably oxygenated ionizable functionalities. As a nonporous solid, the surface area is quite low (1-2  $m^2/g$ ), compared to 50-200  $m^2/g$  found in porous silicas and 100-600  $m^2/g$  for carbon blacks.

The published chromatographic applications of diamond are limited. For example, Josefa *et al* have incorporated a horizontal diamond attenuated total reflection (ATR) element in a flow through cell with low dead volume and used for on-line mid-IR detection in high performance liquid chromatography. They reported that the chemical inertness of the ATR element permits the use of a strongly acidic mobile phase in an isocratic separation [87]. Its hardness allows it to bear high pressures for application in ultra high pressure liquid chromatography. Telepchak has compared the retention of some organic species on columns packed with 10  $\mu m$  natural diamonds to that on conventional  $C_{18}$  bonded phase and finds them similar [10].

Factors that affect the preparation of diamond-packed columns such as volume of slurry solvent, packing pressure, sonication, surfactant solution have been studied by Katinonkul in 2003 [88]. She found that gravitational sedimentation followed by consolidation at high pressure produced good packing conditions. Katinonkul also

reported isotherms for benzyl alcohol, o-, m-, and p-cresol on diamond but the precision of these measurements is questionable, due to the limited column volumes available to her.

### *Crystalline Surface Types*

Crystallographic directions are fabricated lines linking nodes (atom, ions or molecules) of a crystal. Crystallographic planes on the other hand are fictitious planes linking nodes. Different directions and planes have different densities of nodes [86]; these dense planes have an influence on the behavior of the crystal:

1. Optical properties: in condensed matter, light "hops" from one atom to the other with Rayleigh scattering; the speed of light therefore changes according to the directions, no matter how close or far the atoms.
2. Adsorption and reactivity: the adsorption and chemical reactions happen on atoms or molecules, they are therefore sensitive to the density of nodes
3. Surface tension: the condensation of a material indicates that the atoms, ions or molecules are more stable if they are surrounded by other similar species; the surface tension of an interface thus changes according to the density on the surface

The Miller index is used to describe planes and directions in a crystal. In case of directions, a Miller index is of the form of  $[u\ v\ w]$  where the integers represent the coordinates of the vector in real space [89].

Example of directions in a crystal is shown in Figure 5 below [90]

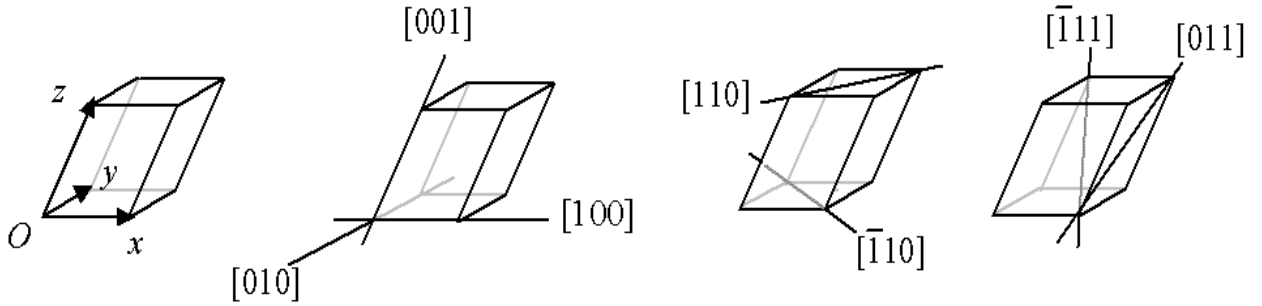


Fig. 5: Directions in a crystal

In the case of planes, a Miller index is of the form  $(h\ k\ l)$  where the integers  $h$ ,  $k$ , and  $l$  represent the  $x$ -,  $y$ -, and  $z$ -intercepts of the plane respectively.

Example of definition of the index for a plane is shown in figure 6 below [91]

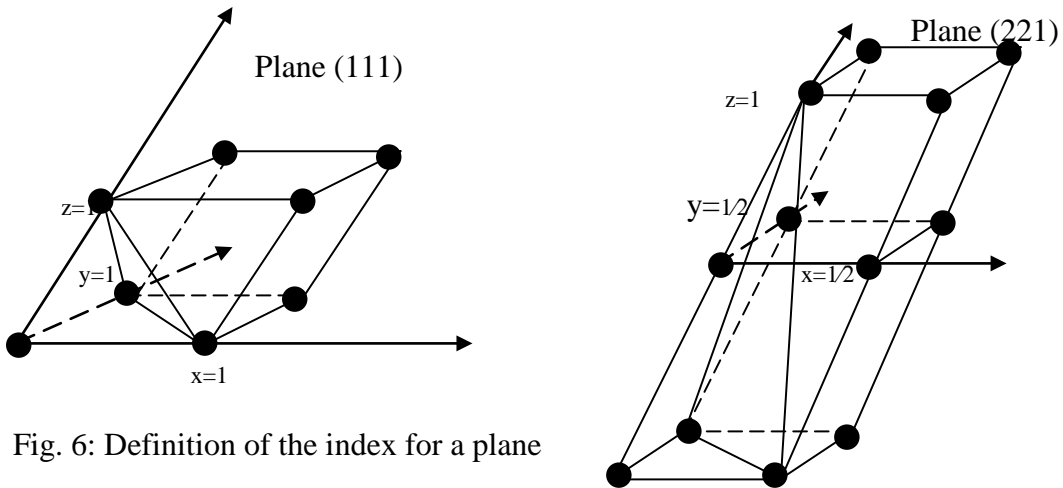
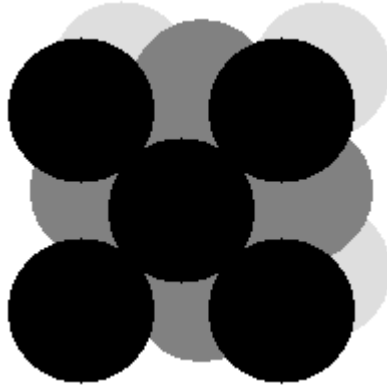


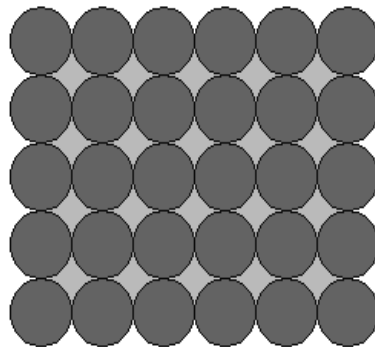
Fig. 6: Definition of the index for a plane

### *The (100) surface*

The  $(100)$  surface is that obtained by cutting the crystal parallel to the front surface of the unit cell - this exposes a surface (the atoms in black) with an atomic arrangement of 4-fold symmetry [92].



Conventional view from above (as shown below) of the (100) surface emphasizes the 4-fold (rotational) symmetry of the surface layer atoms [92, 93].



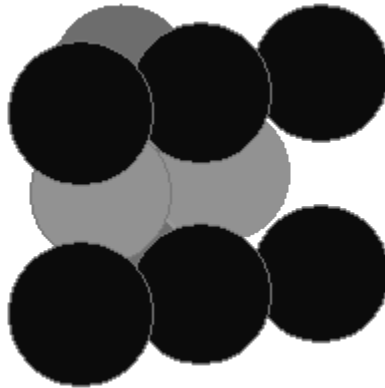
The tops of the second layer atoms are just visible through the holes in the first layer, but would not be accessible to molecules arriving from the gas phase. The following are also worth noting. This means the surface is relatively smooth at atomic level. Such surfaces offer three classes of adsorption sites:

- On-top sites (above a single atom)
- Bridging sites, between two atoms
- Hollow sites, between four atoms

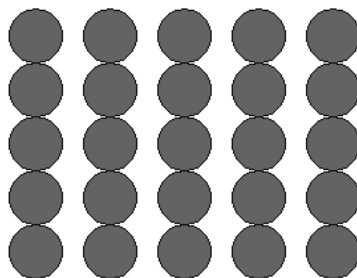
Depending upon the site occupied, a solute (with a single point of attachments to the surface) is therefore likely to be bonded to either one, two or four atoms.

*The (110) surface*

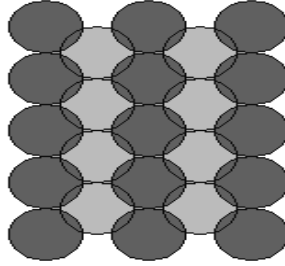
The (110) surface is obtained by cutting the unit cell in a manner that intersects the  $x$  and  $y$  axes but not the  $z$ -axis - this exposes a surface with an atomic arrangement of 2-fold symmetry [92, 93].



The conventional birds-eye view of the (110) surface is shown below. This figure emphasizes the rectangular symmetry of the surface layer atoms [92, 93].



It is clear from this view that the atoms of the topmost layer are much less closely packed than on the (100) surface and that the atoms in the underlying second layer are also, to some extent, exposed at the surface as shown below[92, 93].

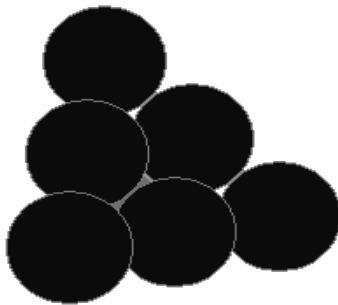


The surface is atomically rough and highly anisotropic and it offers a wide variety of possible adsorption sites, including:

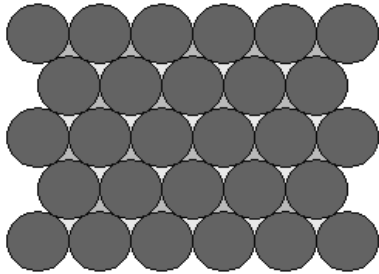
- On-top sites
- Short bridging sites between two atoms in a single row
- Long bridging sites between two atoms in adjacent rows
- Higher coordination sites

### *The (111) surface*

The (111) surface is obtained by cutting the crystal in such a way that the surface plane intersects the  $x$ -,  $y$ - and  $z$ - axes at the same value - this exposes a surface with an atomic arrangement of 3-fold ( apparently 6-fold, hexagonal ) symmetry. This layer of surface atoms actually corresponds to one of the close-packed layers [92].



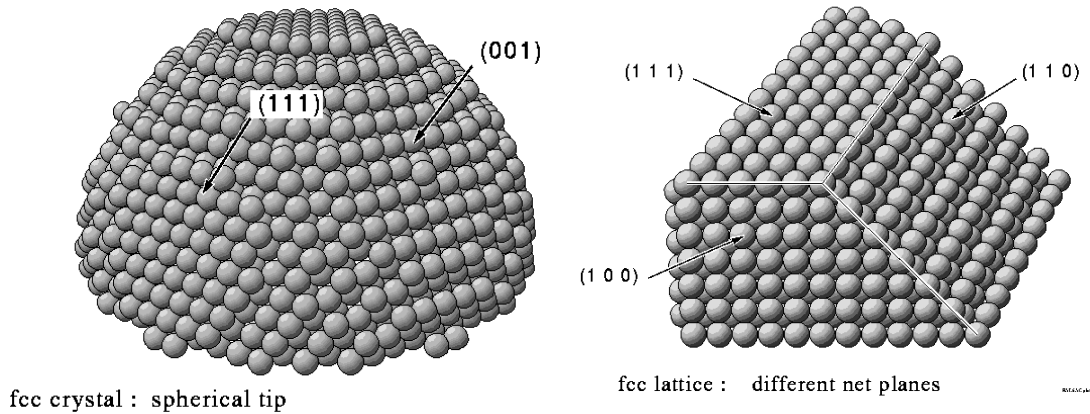
The diagram below shows the conventional birds-eye view of the (111) surface - emphasizing the hexagonal packing of the surface layer atoms. Since this is the most efficient way of packing atoms within a single layer, they are said to be "close-packed".



The surface is almost smooth at the atomic scale offers the following adsorption sites

- On-top sites
- Bridging sites, between two atoms
- Hollow sites, between three atoms

Flat surfaces, therefore are of single crystal samples corresponding to a single Miller Index plane and, each individual surface has a well-defined atomic structure. It is these flat surfaces that are used in most surface science investigations, but it is worth to consider what types of surfaces exist for an irregular shaped sample (but one that is still based on a single crystal). Such samples can exhibit facets corresponding to a range of different Miller index planes. This is best illustrated by the diagrams below [94].



### *Diamond's Surface*

Diamonds (both micro and nanocrystalline), especially those produced by chemical vapor deposition (CVD), have been reported to have hydrophobic surfaces. One indication of this is that these diamonds have a contact angle of  $74.0^\circ$  with water [95]. The low-index (111) surface is of particular interest because it is the natural cleavage plane for diamond, and is thus presumably the most common form present in the material under investigation. The (111) surface is also nearly atomically smooth. Surface atoms restructure into a  $2 \times 1$  reconstruction on a clean surface, giving a C-C nearest neighbor distance of 0.143 nm, nearly identical to that found in graphite (0.1425 nm). At low temperature, the (111) surface of polished diamond crystals show  $1 \times 1$  low-energy electron diffraction pattern, which is related to a hydrogen-covered truncated-bulk geometry [96]. Different bonding models have been proposed for diamond surface. Predominant models among these are dimerization of the surface chains and undimerized  $\pi$ -bonded chains with a slight buckling of the surface chains. By means of energy- and force-minimization computations Scholze *et al* [97] found that the  $\pi$ -bonded chain model

has the minimum-energy structure on the single-dangling-bond cleavage (polished) surface.

It has been found in a preliminary work by Amy Hamsher [98] that the surface of diamond contains at least three (3) different classes of ionizable species. It has been reported that diamond's surface can be occupied by molecular oxygen [99]. Bobrov et al [99] attributed this to surface defects. Interestingly, single dangling bonds can exist in the vicinity of hydrogen-related defects [100].  $\pi$ -bonded carbon-carbon dimers are not reactive with molecular oxygen [99]. Nitrogen-doped diamonds exist in nature and now because of electronic application inclusion of stable dopands (e.g. nitrogen) within diamond grown by CVC is very common [101]. Barnard *et al* [102] report that the nitrogen is likely to be positioned at the surface of both hydrogenated nanodiamond and (dehydrogenated) "bucky-diamond."

## CHAPTER THREE

### EXPERIMENTAL PROCEDURE

#### Materials

Columns studied in the research were packed with synthetic diamond (size of about 4-8  $\mu\text{m}$ ) from ADAMAS Laboratory Corporation (Windsor, Canada). Method of packing is described elsewhere [11].

Sodium nitrate (granular – Mallinckrodt Chemical Works), sodium sulfite (anhydrous, certified A.C.S – Fisher Scientific), sodium thioisulphate (anhydrous – EM Sciences), uracil (prepared and characterized by Dr. Kyler, IUP) were used as void volume markers and acetone (research grade) was utilized in the isotherm determination. Methanol (Fisher Scientific) was one of the mobile phase constituents. Deionized-water was in-house, reverse osmosis purified, treated with a Milli-Q<sup>TM</sup> system (Millipore, Inc., Bedford, MA, USA). Potassium chloride (“Baker Analyzed” reagent) was also used as one of the mobile phase constituents to increase the ionic strength of the mobile phase.

#### Equipment and Instrumentation

Columns were slurry packed by means of a Haskell pump (Altech, Deerfield, IL, USA).

Frontal analysis was performed with a Model 222C HPLC pump (SSI), a Model 500 Variable-Wavelength UV/Vis Detector (SSI) and Model 3390A Integrator (Hewlett Packard), with waters Automated Gradient Controller. The column temperature was controlled by a Model 900 Isothemp refrigerated Circulation water bath (Fisher Scientific). The temperature was measured to  $\pm 0.1$  with a thermometer.

## Procedure

Efficiency of column was evaluated by collecting retention data of solute solutions at room temperature under isocratic conditions with mobile phase flow rate of 0.5 mL/min. The mobile phase was 50% (v/v) methanol in water and the UV detector was used at wavelength 254 nm. The retention time of each solute was evaluated at the peak maximum and then the retention factor,  $k$  was calculated based on the void volume ( $V_m$ ).

$V_m$  was determined by the utilization of the “retention time” of neutral (uracil) and ionic (e.g.  $\text{NaNO}_3$ ) compounds. Here, the mobile phase was 50% (v/v) methanol in water for uracil analysis and 0.1 M (or 80 mM) KCl in 50% (v/v) methanol in water.

## Isotherm Measurement

Frontal analysis was used to determine all the equilibrium isotherms. Series of concentrations of the solute were prepared by diluting in the mobile phase, a mixture of 50% (v/v) methanol in water. The amount of the solute (acetone) on the surface at equilibrium was determined from the breakthrough curve for the concentration.

## Thermodynamic Parameter

Enthalpy change ( $\Delta H$ ) associated with the adsorption process was determined from the retention data of acetone collected at different temperatures at a flow rate of 0.5 mL/min. The mobile phase was 50% (v/v) methanol in water. Measurements were made in triplicates.

## CHAPTER FOUR

### RESULTS AND DISCUSSION

Diamond particles are non porous, hence only interstitial space is available for fluid to flow through diamond packed columns. The fluid element must then dodge from side to side in order to avoid the solid matter in their path. Such tortuous flow is very irregular. Thus by any measure, the microscopic flow through a granular material is unpredictable and capricious; and the flow displacement is best thought of as a random process.

The effective particle size (calculated from the pressure drop and flow rate data using eqn 4-1 [103]) is 3.2  $\mu\text{m}$  (instead of manufacturer's 5 $\mu\text{m}$ ). Small particles such as this pack together more tightly than large particle do, and present considerable resistance to fluid motion. In order to maintain a reasonable analysis time, the flow rate was kept at 0.5 mL/min, which resulted in a pressure drop of about 900 psi. Even at this high pressure drop, the reduced velocity (ratio of mobile phase velocity to the velocity of the solute diffusion through the column) of the mobile phase was found to be about 6, which lies within the high performance regions of column.

Concerning particle size and its associated pressure drop, a formal study was conducted to assess the cause of the difference between our calculated particle size (3.2  $\mu\text{m}$ ) and the manufacturers reported value (5  $\mu\text{m}$ ): manufacturer reporting the “wrong” value or the diamond particle are being wetted during the experiment. For this, various solvents (see Table 1) were employed. The effective particle size (average) as obtained from each of the solvents are as reported in Table 1 and was calculated using the Kozeny-Carman equation,

$$d_p = \sqrt{\frac{180L^2\eta(1-\varepsilon)^2}{\Delta P\varepsilon^2t_M}} \quad \text{Eqn 4-1}$$

where  $d_p$  = effective particle size

$L$  = column length (cm)

$\Delta P$  = pressure drop across the column (note, 1 psi = 689476 dyne/cm<sup>2</sup>)

$\eta$  = viscosity (Poise, P = sec.dyne/cm<sup>2</sup>)

$\varepsilon$  = fraction of unoccupied space (porosity, minimum of 0.4)

Table 1. Particle size as obtained from different solvents

Solvent	Density g/mL	Viscosity cP	Surface Tension dyn/cm	Effective Particle size µm
Water	0.9982	1.000	72.8	3.3
2-Propanol	0.7854	2.400	21.7	3.8
Ethanol	0.7893	1.194	22.8	4.3
Methanol	0.7913	0.550	22.5	2.9
Acetone	0.7900	0.360	23.32	2.5
Acetonitrile	0.7822	0.380	19.1	2.1
Hexane	0.6594	0.31	18.400	2.8

As is evident from Figure 7 and Table 1, properties such as density and surface tension of the solvents do not have observable effect on the particle size; hence wetting of the column by these solvents can be ruled out. This simply means that the cohesive force between diamond and these solvents is not defined or regular. However, viscosity and kinematic viscosity (absolute viscosity divided by density) did have an effect on the particle size, as can be inferred from Kozeny-Carman's equation. Thus, the type of solvent which is employed as the mobile phase can influence the experimentally observed

particle size since the actual flow rate and pressure drop will differ from solvent to solvent based on the solvent's viscosity.

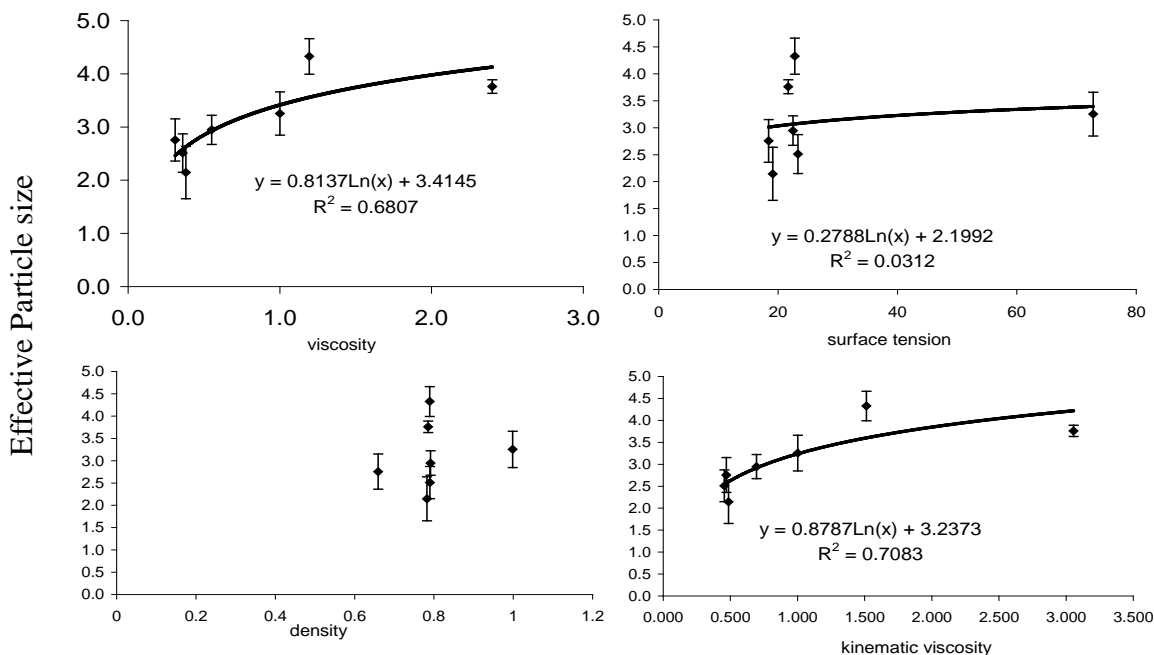


Figure 7. Effective particle size versus a property of solvent used Note: kinematic viscosity is the absolute viscosity divided by density

### Void Volume ( $V_m$ )

The seemingly simple process of measuring the mobile phase volume (i.e. the void volume, also known as the hold up volume) in reverse phase liquid chromatography has eluded unambiguous agreement over the century. Examples exist in the literature where the reported void volume is physically impossible, either equal to or larger than empty column volume [104], or being so small that it would represent a total porosity of half the theoretical limit for well-packed columns [105].

For non porous particles, such as that used for this study only 40% of the volume of the container is supposed to be void after packing. This calculation gives a 5.73 mL void volume of the 300×7.8 mm ID column used.

Various methods were employed to ascertain the correct hold up volume. Among them, the use of unretained components (inorganic salts) seemed to give values closest to the predicted value (5.73 mL). As previously predicted by Hamsher [98] and other researchers [99, 100], the surface of diamond contain some ionizable groups (e.g. carbonate and pivalic acid). The electrostatic charges of these groups possibly exclude ionic substances (Donnan effect), making the measured void volume smaller than expected. The observed values are shown in Table 2.

One way to overcome Donnan effect would be to protonate these ionizable surface groups. To do this, 50% methanol in water with 0.5 mL H<sub>3</sub>PO<sub>4</sub> per liter was employed as the mobile phase. The results are also shown in Table 2. The void volume increased but not as expected. Further, smaller species are expected to occupy most of the pores and hence spend more time in the column than bigger ones. The opposite was observed: bigger ions (S<sub>2</sub>O<sub>4</sub><sup>2-</sup>) gave bigger void volumes than smaller (NO<sub>3</sub><sup>-</sup>) ones (see Table 2, second row).

Table 2. Void volume of diamond packed column as measured with different solutes in 50% methanol in water, with and without H<sub>3</sub>PO<sub>4</sub>, and with different amounts of KCl

Mobile Phase	Solute (radius*)		
	Thiosulfate (230 pm)	Sulfite (200 pm )	Nitrate (170 pm)
50:50 MeOH:H <sub>2</sub> O	5.28 mL	5.31 mL	5.16 mL
50:50 MeOH:H <sub>2</sub> O with 0.5 mL H <sub>3</sub> PO <sub>4</sub>	5.65 mL	5.62 mL	5.53 mL
50:50 MeOH:H <sub>2</sub> O with 50 mM KCl	5.67 mL	5.26	5.42
50:50 MeOH:H <sub>2</sub> O with 80 mM KCl	5.32	5.66	5.77
50:50 MeOH:H <sub>2</sub> O with 100 mM KCl	-	5.68	-

\*Thermochemical radii were estimated using method by Correa H. S. et al (J. Chem. Edu., 1987, 62 942)

This may indicate incomplete protonation of the ionized diamond surface, with the residual charged groups accounting for the repulsion of ionic species and their subsequent inability to penetrate the hydrophobic structure of the stationary phase. Another method of reducing Donnan effect is to increase the mobile phase ionic strength. For this, mobile phases with different ionic strengths (50 mM, 80 mM and 100 mM KCl) were prepared. These data are also shown in Table 2. Under these conditions, smaller ions showed void volumes consistent with expectations, while larger ions show lower than expected void volumes. The measured void volumes increased with increasing ionic strength until mobile phase with 100 mM KCl, which did not give any significant difference from that obtained from 80 mM KCl.

In an attempt to determine the correct void volume, uracil was also employed, but was observed to be retained on diamond surface.

In order to test the performance of our column, retention data for both ionic and neutral (uracil) solutes were collected at different temperatures. Ionic species showed essentially no variation in retention volume with temperature but uracil did (data not shown). From this, we were able to calculate the enthalpy change associated with the adsorption of uracil on diamond surface, which is discussed later.

From Table 2, the following implications about our diamond packed column can be inferred:

- There are interstitial holes and/or fissures within the particles which are bigger than 230 pm and there are others that are less than 170 pm (Table 2).
- The nature of the surface is influenced by the pH and ionic strength of the mobile phase.

- Not only is the chemical nature of solutes important but also the size of the solute adsorbed onto the surface of the diamond packed column plays a major role in the solute's adsorption process.

It is known that pore size distribution and accessible surface area of chromatographic adsorbents control intraparticle diffusion, capacity and dynamic binding capacity [106, 107]. In our case, interparticle space sizes are likely to have a great influence on the above mentioned properties of the column.

Since the presumably unretained inorganic solutes gave the closest results to the calculated void volume (5.73 mL), the true and experimental void volume was estimated to the average of the all void volumes obtained in Table 2, which turned out to be 5.47 mL. However, the following summary can be made about the individual void volumes reported in Table 2. The use of 50/50 MeOH/H<sub>2</sub>O with 0.5 mL H<sub>3</sub>PO<sub>4</sub> gave higher void volumes than just 50/50 MeOH/H<sub>2</sub>O as mobile phase because of the reduced repulsive forces by the ionized functionalities present on the surface of diamond that exclude these inorganic solutes. The presence of H<sup>+</sup> ions covers the negatively charged functional groups. It is also evident from Table 2 that void volume increased with ionic strength of the mobile phase. It is also true that the monovalent anion generally gave values higher than the highly charged anions. Mobile phase with higher ionic strengths gave high void volumes because at higher ionic strength, the inorganic void volume markers had full access to the most of the free spaces of the stationary phase and gave the maximum hold-up time of the column.

## Column Efficiency

As it has been explained earlier, the efficiency of a column is expressed in the form of number of theoretical plates (N). It is the ratio of the square of the center of mass of the peak to the variance of that peak; hence, larger values of N express small amount of variance or band spreading, during the time of the solute retention within the column.

The plate count for commercially available columns ranges within thousands or even low tens of thousands for columns of this size. Table 3 below summarizes the plate count obtained for our column for different solutes.

Table 3. Efficiency of diamond packed column according to solute

<b>Solute</b>	<b>Plate count (N)</b>
NaS <sub>2</sub> O <sub>4</sub>	368
Na <sub>2</sub> SO <sub>3</sub>	449
NaNO <sub>3</sub>	387
Acetone*	124
Benzyalcohol*	38
Uracil*	84

\* retained on diamond

It is apparent that all the N values are smaller than commercially available columns, but it is in agreement with previous data that have been obtained on diamond pack columns [85]. These small N values are very surprising because the measured void volume is very much in agreement with what is expected, which indicate that the column

is “well packed”. It has been reported by Schure and Maire [108] that efficiency can vary depending on subtle details of the packing. For example, they reported that for a particle pack where 6% of the particles are removed from the pack, 33% of the column efficiency is lost. Hence, they concluded that, “it is advisable that when packing a column, it is more important to prevent defect sites leading to inhomogeneous packing rather than obtaining the highest density pack with the smallest interstitial void volume”. It appears that although the packing density was good, there were nonetheless a high number of “defect sites” in the column bed. While such poor chromatographic efficiency may be acceptable for frontal analysis studies of adsorption thermodynamics, it is unacceptable for most chromatographic methods of isotherm measurement, let alone any serious chromatographic work.

Further, the fact that all unretained solutes had similar plate count (hundreds) but the retained ones varied greatly suggest that there is a geometrical factor due to the heterogeneity of the diamond surface. Thus, the surface bonds or adsorbs different solutes to different extents and/or with different mechanism.

It is also apparent that the “unretained” solutes all show higher efficiencies while the most retained ones (uracil and benzyl alcohol) show the smallest plate counts. This may suggest that there is a significant mass transfer, most likely from the kinetics of desorption of solute from the stationary phase.

### Adsorption Isotherm

To assess adsorption mechanism, adsorption data was systematically measured by frontal analysis (FA). Acetone was chosen for this investigation because it has an

exceptionally high solubility in methanol-water solutions. Such high solubility allow that FA measurement be carried out under such conditions that the adsorbed concentration become close to the monolayer saturation capacity of the column.

Figure 8 shows the resultant adsorption data for acetone, without fit to any isotherm model. That is, the lines shown are simply to emphasize the trend in the data set.

Generally, the trends lack consistency as would have been expected for temperature dependent measurements, that is the data for the highest temperature falls between that of the lowest and middle temperature.

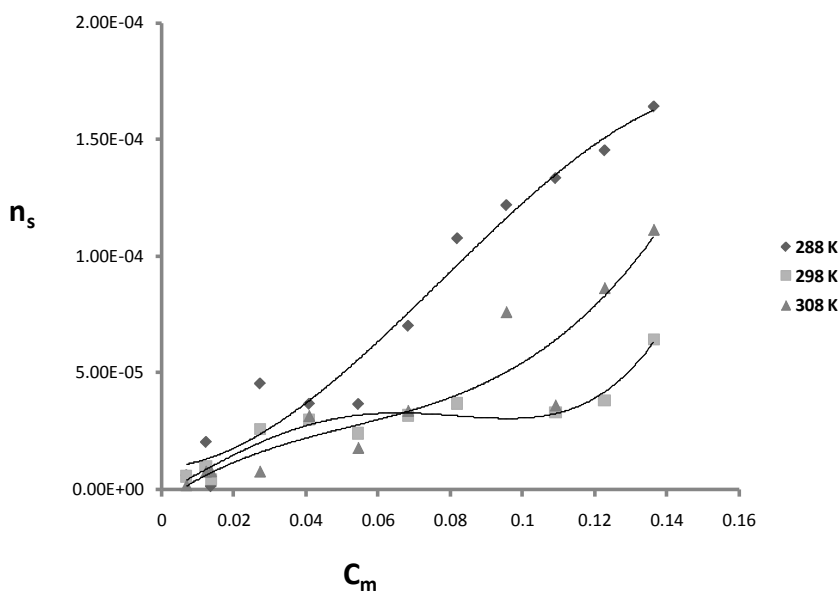


Figure 8: Adsorption data for acetone without fit to any isotherm.

However, three things are certain from the data:

- a) they show temperature sensitivity and they are all linear at low concentration (Fig. 8). This means that at low concentration, all of the solutes are adsorbed on a single class of adsorption site and effectively adsorbing independently. This can suggest monolayer coverage at low concentrations, irrespective of the temperature (Fig. 9).

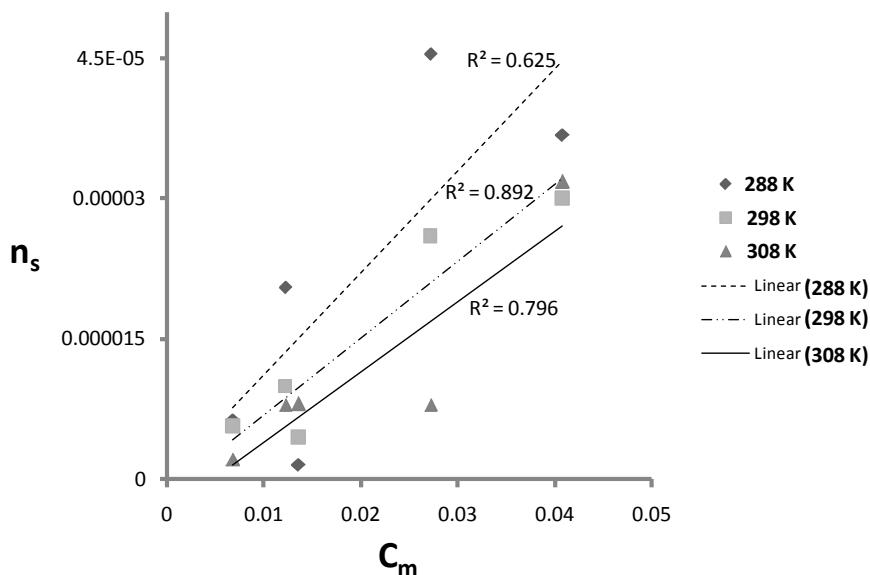


Figure 9: Low concentration part of Fig.8 with linear trend.

The slopes of these lines give the equilibrium constant, which in turn offer the enthalpy ( $\Delta H$ ) change and entropy change ( $\Delta S$ ) associated with adsorption of acetone on diamonds. The calculated  $\Delta H$  is  $-40 \text{ kJ.mol}^{-1}$ , and  $\Delta S$  is found to be negative (actual value of  $\Delta S$  is unknown because of the unknown phase ratio).

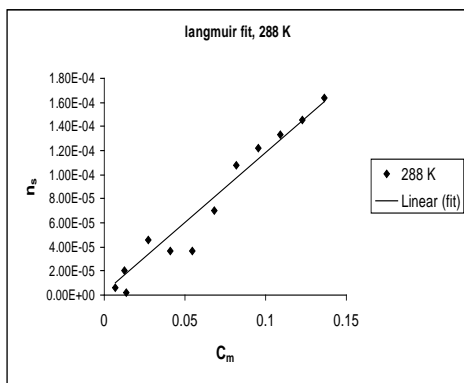
b) The shape of the isotherm at 288 K is significantly different from that of the higher temperatures (298 and 308 K) – Figure 8.

c) There appear to be two plateaus, one at low concentration and the other at high concentration in all isotherms, but being very pronounced at high temperatures.

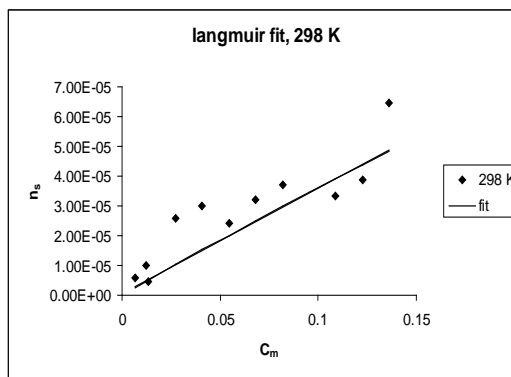
One isotherm model that assumes monolayer coverage is the Langmuir isotherm. It is interesting to note that experimental isotherm data generated at 288 K fit reasonably well to the Langmuir isotherm (fig. 10a) while the other temperatures did not (fig. 10b & c). It is therefore proper to imply that there is a shift from monolayer behavior at low

concentrations to something else (probably multilayer behavior) at high concentrations for isotherm obtained at both 298 and 308 K.

a)



b)



c)

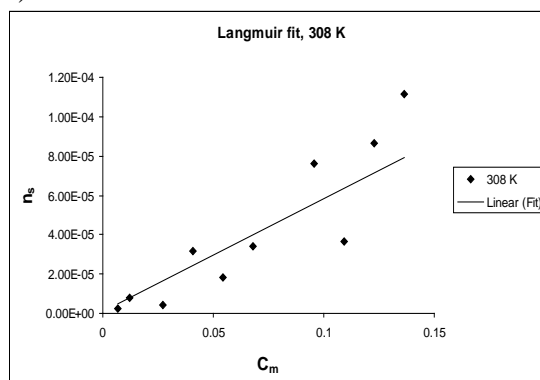


Figure 10. Fit of experimental data to Langmuir Isotherm.

- a) 288 K ( $a = 0.00126$ , and  $b = 0.6003$ ), b) 298 K ( $a = 0.00038$ , and  $b = 0.525$ ),  
 c) 308 K ( $a = 0.000615$ , and  $b = 0.525$ )

Therefore, adsorption of acetone onto diamond surface where all active sites are assumed to be equivalent with no acetone-acetone interactions appears to have failed in this work. This gives room for us explore other adsorption mechanisms. However, to proceed, one needs to understand the various mechanisms by which solutes are adsorbed onto a surface.

Two mechanisms have been proposed to be operative in reverse phase liquid chromatography: adsorption and partition. From the structure of the surface of diamond, a partition mechanism can be ruled out in this experiment. In adsorption, it has been shown that retention is primarily due to hydrophobic interactions between the mobile phase and the solute [17, 109].

A major reason why we are seeing a change in the shapes of the isotherms between 288 K and the higher temperatures has been suggested to be due to the break of hydrophobicity at high temperatures. Frank and Evan [110] have modeled the hydrophobic effect from the structure of water. They stated that at low temperature water molecules surrounding a non-polar solute adopt orientations (low energy) to avoid wasting hydrogen bonding; while at high temperature more conformations become accessible (high entropy), but at the cost of breaking hydrogen bonds. They then concluded that hydrophobicity is entropic at low temperature and enthalpic at high temperature.

Thus, the change in shape can be said to come from two or more different mechanisms operating at different temperatures at diamond's surface, since hydrophobicity, the main driving force of adsorption onto diamond surface is thought not to be operative at high temperatures.

As discussed earlier, the low concentration side of all isotherms appeared to be Langmuirian. Hence thermodynamic parameters for the adsorption of acetone were calculated from the equilibrium constant of the Langmuir equation, i.e.  $a = K$ . The enthalpy change obtained from this was - 40 kJ/mol and entropy change was observed to be negative. From these values and  $\Delta G = \Delta H - T\Delta S$ , the process of adsorbing acetone

onto the surface of diamond is favorable only at low temperatures and it very much depends on entropy. The process is exothermic. It is therefore not surprising that the isotherm generated at 288 K fitted reasonably well to the Langmuir isotherm. Also, the monolayer coverage assumption at low concentrations is valid because parameter “a” (0.00126) in the Langmuir isotherm obtained from fitting of the 288 K data to the Langmuir model is very much in agreement with the slope (0.0012) for the low concentration side of the 288 K isotherm.

Two things are therefore proposed to be occurring during adsorption of acetone onto diamond surface at high temperatures: multiple layer coverage or different adsorption site are activated enough at high temperature to react differently. There are at least four reasons why these proposals may be valid:

1. From the thermodynamic parameters calculated ( $\Delta S$  and  $\Delta H$ ), the adsorption of acetone onto surface of diamond is not favorable at high temperatures
2. Hydrophobicity, which is the driving force for the adsorption of solutes onto diamond surface, is evidently not in operation at high temperatures.
3. Variable plate counts have been obtained for different solutes, suggesting the presence of surface defects or multiple surface adsorption sites.
4. The supposed monolayer coverage of diamond by acetone corresponds to about  $4400 \text{ \AA}^2$  of area for each acetone molecule. This area of acetone is incredibly big to be true. However, this may be accounted for by assuming multiple sites at the surface of diamond, which is explained later. This area ( $4400 \text{ \AA}^2$ ) was obtained by noting the volume of the column occupied by the diamond particles (8.98 mL, empty volume – void volume). With the density of diamond is (3.53 g/mL), the

total mass (grams) of diamond used for the packing was calculated. By assuming that each gram of diamond occupies  $1 \text{ m}^2$ , and knowing the amount of acetone at monolayer is about  $6.0 \text{ } \mu\text{mol}$ , the area corresponding to this amount was calculated.

Based on these observations, the collected data were also fitted to different adsorption isotherm models:

- Those that assume multiple layer coverage and
- Those that assume multiple sites.

The quadratic isotherm model was chosen to account for multiple layer coverage situation. Isotherms described by this model are concave upwards at low concentration. This has been attributed to strong adsorbate-adsorbate interactions. Figure 11 below show how the generated data fit to the quadratic isotherm model. It is seen that the isotherm at 308 K fit better than at 298 K (indicated by error bars), and this could be due to the fact that adsorbate-adsorbate interactions is expected to increase with temperature. Hence at 298 K, there is not enough drive for these interactions. The adjustable parameters,  $b_1$  and  $b_2$  for these isotherms are 0.000345 and  $7.25 \times 10^{-5}$  respectively for 308 K and  $7.9 \times 10^{-6}$  and 0.0270 respectively for 298 K. Attempts were made to increase the adjustable parameters from two (2) to three (3) but did not change the shapes of the isotherms. The experimental data were also fitted to the BET isotherm model, another multilayer isotherm model, but the result was no better than the quadratic.

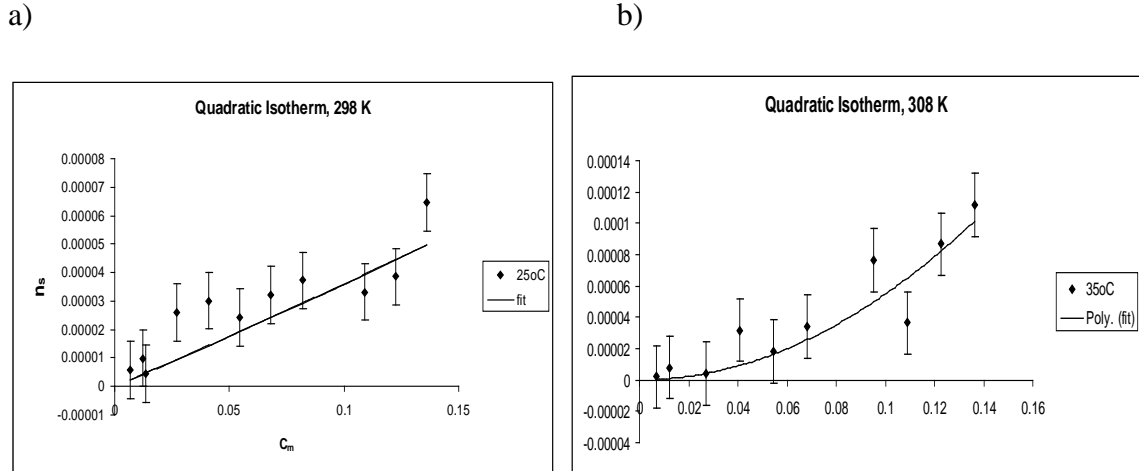


Figure 11: Fit of experimental data to quadratic isotherm model: a) 298 K, b) 308 K

The Bi-Langmuir isotherm model however, takes into account surface heterogeneity, especially surface coverage with two different kinds of chemical groups. Experimental isotherm data generated at 298 K fitted better than at 308 K, however the spread in each case were substantial (fig 12) and could mean that there is no such multiple site contributing to the adsorption process.

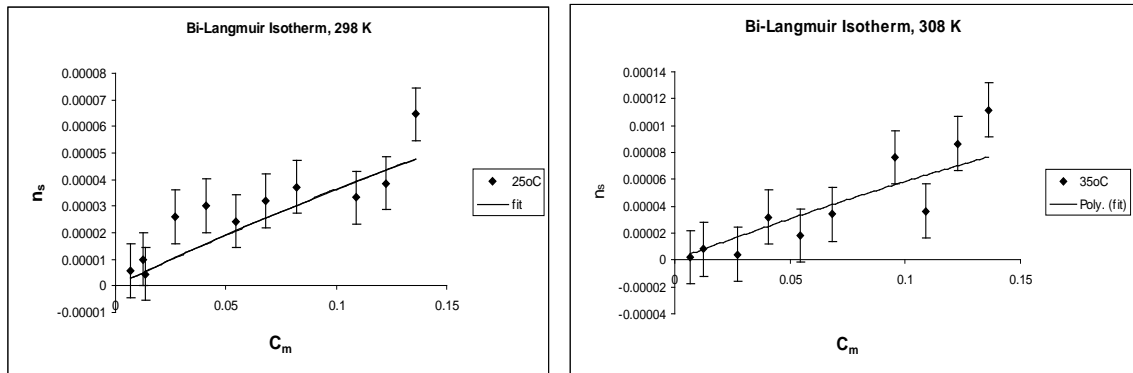


Figure 12: Fit of experimental data to Bi-Langmuir Isotherm model: a) 298 K, b) 308 K

Afzal *et al* (1998) [111] have studied the adsorption of acetone on activated carbon in the gas phase at low temperature. The adsorption isotherm was found to be Langmuirian. The associated enthalpy change during the adsorption process was observed to be -34 kJ/mol. This is in good agreement with the -40 kJ/mol obtained for

adsorption of acetone on diamond. The difference may be due to the different phases of environments employed in each experiment – solvated versus free molecules. The enthalpy change associated with the adsorption of uracil on diamond surface has been found to be - 20.19 kJ/mol.

For acetone adsorbed from solution (carbon tetrachloride) onto a fully hydroxylated silica surface, two IR-absorption bands for carbonyl stretching vibration were recorded at  $1690\text{ cm}^{-1}$  and  $1705\text{ cm}^{-1}$  [112]. The former was found at low acetone concentration in solution and corresponded to a stronger adsorption mode where, in the authors' opinion, an acetone molecule is involved in hydrogen bonding with two adjacent hydroxyl groups. The weaker adsorption mode (at  $1705\text{ cm}^{-1}$ ) was assigned to hydrogen bonding between isolated OH-groups and acetone.

In 1998, Okunev *et al* [113] studied interaction of acetone with fully or partially hydroxylated surfaces of a KSS-3 silica gel in the gas phase. Their adsorption isotherm also showed two plateaus. IR absorption band showed two CO bands which are in close connection. These authors then concluded that there are two adsorption complexes of acetone with different hydroxyl (OH) groups of silica.

Indeed from Figures 8 and 13, two plateaus are seen in all the isotherms, but very prevalent at higher temperatures. Here we infer that the two plateaus observed are caused by chemical irregularity of the diamond surface and correspond to acetone adsorption on different surface centers, but not necessarily with OH groups.

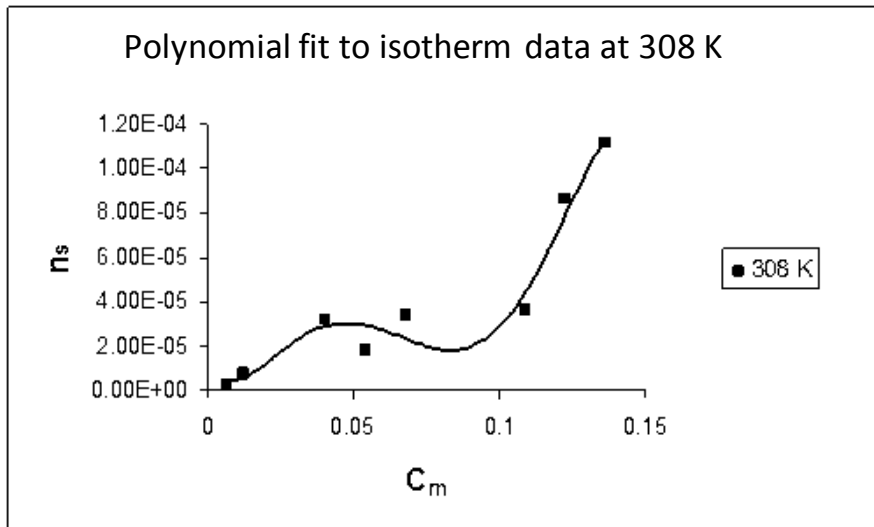


Figure 13: Example of two plateaus seen in adsorption isotherms of diamond.

The abnormally high surface area of the monolayer observed in this experiment is not uncommon in literature, especially in cases where two plateaus are seen [114]. This has normally been expressed in the form of higher fractal dimension. This situation has been partly attributed to wrongly considering the first plateau as corresponding to monolayer adsorption because there is a chance that acetone concentration will change in a very narrow range during the isotherm measurement. An alternative and perhaps plausible explanation has been given by Van Danne *et al* [115]. They explained that since adsorbed molecules do not occupy only places on the surface, but also neighboring volumes, they create steric difficulties for adsorption of other molecules and leads to overestimation of the surface of the monolayer.

## CHAPTER FIVE

### CONCLUSIONS

Efficiency of the diamond packed column was found to agree generally with the previous works on diamonds, but showed marked variation for retained compounds. This has been attributed to surface defects. It is therefore recommended that ways must be devised to prevent site defects when packing columns of high density. Otherwise, it is more important to reduce site defects when packing than obtaining the highest packed column with small void volume.

Retention of acetone on diamond has been found to have similar enthalpy change as those on activated carbon. The process is exothermic on both adsorbents.

Both retention and isotherm results confirm the presence of ionizable groups at the surface of diamond particles produced by chemical vapor deposition

Acetone adsorption on diamond has been found to be sensitive to temperature, for which low temperature adsorption appears to be Langmuiring. The isotherm results, in general show two plateaus, one at low concentration and the other at high concentration. This has been associated with complexes of acetone with different surface groups.

The abnormally high size of the monolayer on the diamond surface has been attributed to complete filling of the first monolayer by the second plateau.

## References:

1. Guiochon, G.; Shirazi, S.G.; Katt, A.M., *Fundamentals of Preparative and Nonlinear Chromatography*, 1994. Academic Press Inc., London, UK. pp 61-83
2. De Vault, D. *J. Amer. Chem. Soc.* 65,1943, 532
3. De Jong, A.W.J.; Kraak, J.C.; Poppe, H. and Nooitgedacht F. *J. Chromatogr.* 193, 1980, 181
4. Conder, J. R. and Purnell, J. H. *Trans. Faradays Soc.* 65,1969, 839
5. Huber, J.F.K and Gerritse R.G., *J. Chromatogr.* 58 ,1971, 137
6. Langmuir, I., *J. Amer. Chem. Soc.*, 38,1916, 2221
7. Jana, M.J.; Frenz J.H. and Horvath C. *Ind. Eng. Chem. Res.* 26 (1) 1987, 43-50
8. Stan, V. *Thin Solid Film* 317 (1-2), 1998, 449-454
9. Krauss, et al *Diamond and Related Materials* 10 (11), 2001, 1952-1961
10. Telepchak, M. J. *Chromatographia*, 6, 1973, 234.
11. Nuamthanum, A. MS thesis, IUP, Indiana, PA, 2002.
12. Lesney, M.S. *Today's Chemist at Work* 7, 1998, 67-72.
13. McCalley, D. V. *J. Chromatogr. A* 1038, 2004, 77-84
14. Horvath, Cs.; Melander, W.; Molnar, I. *J. Chromatogr.* 125, 1976, 129-156
15. Horvath, Cs.; Melander, W. *Am. Lab.* 1978, 17-36
16. Martire, D.E.; Boehm, R.E. *J. Phys. Chem.* 87, 1983, 1045-1062
17. Dill, K.A. *J. Phys. Chem.* 91, 1987, 1980-1988
18. Yink, P.T.; Dorsey, J.G.; Dill, K.A.; *Anal. Chem.* 61, 1989, 2540-2546
19. Cole, L.A.; Dorsey, J.G *Anal. Chem.* 62, 1990, 16-21
20. Grushka, E.; Colin H.; Guiochem, G. *J. Chromatogr.* 248, 1982, 325-339
21. Sander, L.C.; Field, L.R. *Anal. Chem.* 52,1980, 2009-2013.

22. Isaaq, H.J.; Jaroniec, M. *J. Liq. Chrommatogr.* 12, 1989, 20067-2082
23. Tchaplá, A.; Heron, S.; Colin, H.; Guiochem, G. *Anal. Chem.* 60, 1988, 1443-1448
24. Hammers, W.E.; Verschoor, P.B.A. *J. Chromatogr.* 282,1983, 41-58
25. Morel, D.; Serpinet, J. *J. Chromatogr.* 200, 1981, 95-104
26. Ying, S.S.; Gilpin, R.K. *J. Chromatogr.* 449, 1988, 115-118
27. Kazakevich, Y. McNair, H. *Basic Liquid Chromatography*,  
[http://hplc.chem.shu.edu/new/hplc\\_book/](http://hplc.chem.shu.edu/new/hplc_book/).
28. van Deemter, J.J. Zuiderweg, F.J. Klinkenberg, A. *Chem. Eng. Sci.* 5,1956, 271-289.
29. Giddings, J.C. *Dynamics of Chromatography: Part 1*, Marcel Dekker, New York, 1965
30. Horvath, C. Lin, H.-J. *J. Chromatogr.* 126, 1976, 401-420.
31. Bristow, P.A. Knox, J.H. *Chromatographia* 10 ,1977, 279.
32. Knox, J.H. *J. Chromatogr. A* 831,1999, 3-15.
33. Poole, C.F. Poole, S.K. *Chromatography Today*, Elsevier Science B.V, Amsterdam, 1991
34. Laeven, J. M ., Smit, H. C. *Analytica Chimica Acta*, 176 (1985) 77-104
35. Knox, J.H. Kaliszan, R. *J. Chromatogr.* 349, 1985, 211.
36. Kazakevich, Y.V. McNair, H.M. *J. Chromatogr. Sci.* 31, 1993, 317.
37. Kazakevich, Y.V. McNair, H.M. *J. Chromatogr. A* 872, 2000, 49.
38. Yun, K.S. Zhu, C. Parcher, J.F. *Anal. Chem.* 67, 1995, 613.
39. Djerki, R.A. Laub, R.J. *J. Liq. Chromatogr.* 10, 1987, 1749.
40. Alhedai, A. Martire, D.E. Scott, R.P.W. *Analyst* 114, 1989, 869.
41. Majors, R.E. Carr, P.W. *LC-GC* 19, 2001, 124.
42. McCormick, R.M. Karger, B.L. *Anal. Chem.* 52, 1980, 2249.

43. Gutnikov, G. Hung, L.B. *Chromatographia* 19, 1984, 260.
44. Möckel, H.J. *J. Chromatogr. A* 675, 1994, 13.
45. Rustamov, I. Farcas, T. Ahmed, F. LoBrutto, F. C. R. . McNair, H.M, Kazakevich, Y.V. *J. Chromatogr. A* 913, 2001, 49
46. Berendsen, G.E. Schoenmakers, P.J. de Galan L., *J. Liq. Chromatogr.* 3, 1980, 1669
47. van der Houwen, O.A.G.J., van der Linden, J.A.A., Indemans, A.W.M. *J. Liq. Chromatogr.* 5, 1982 2321
48. Stanley, B.J. Foster, C.R. Guiochon, G. *J. Chromatogr. A* 761, 1997, 41.
49. Bidlingmeyer, B.A. Warren, F.V. Weston, A. Nugent, C. *J. Chromatogr. Sci.* 29,1991, 275
50. Nowotnik, D.P. Narra, R.K. *J. Liq. Chromatogr.* 16, 1993, 3919.
51. Fini, O. Brusa, F. Chiesa, L. *J. Chromatogr.* 210, 1981, 326.
52. Didaoui, L. Touabet, A. Ahmed, A.Y.B.H. Meklati, B.Y. Engerwald, W. *J. High Resolut. Chromatogr.* 22, 1999, 559
53. Smith, R.J. Nieass, C.S. Wainwright, M.S. *J. Liq. Chromatogr.* 9, 1986, 1387.
54. Popl, M. Voznakova, Z. Tatar, V. Strnadova, J. *J. Chromatogr. Sci.* 21, 1983, 39-42
55. Vít, I. Fähnrich, J. Popl, M. *Collect. Czech. Chem. Commun.* 54, 1989, 953.
56. Jinno, K. Ozaki, N. Sato, T. *Chromatographia* 17, 1983, 341.
57. Wells, M.J.M. Clark, C.R. *Anal. Chem.* 53, 1981, 1341.
58. Engelhardt, H. Müller, H. Dryer, B. *Chromatographia* 19,1984, 240.
59. Oumada, F.Z. Rosés, M. Bosch, E. *Talanta* 53, 2000, 667.
60. Krstulovic, A.M. Colin, H. Guiochon, G. *Anal. Chem.* 54, 1982, 2438.
61. Kazakevich, Y.V. McNair, H.M. *J. Chromatogr. Sci.* 33,1995, 321.
62. Vít, I. Popl, M. Fähnrich, J. *J. Chromatogr.* 281, 1983, 293.

63. Carr, L. Li, P.W., Evans, J.F. *J. Chromatogr. A* 868, 2000, 153.
64. Rosés, M.; Canals, I.; Allemann, H.; Siigur, K.; Bosch, E. *Anal. Chem.* 68,1996, 4094.
65. Langmuir J. *J. Amer Chem. Soc.* 1917, 39 1848-1906
66. Jovanovic D.S. *Kolloid-Z. Z. Polym.*, 1969, 235, 1203-1213
67. Melander, W.R.; Erard J.F. and Horvath C.S. *J. Chromatogr.* 282, 1983, 211
68. Andrade, J.D. in *Surface and Interfacial Aspects of Biomedical Polymers*, Andrade J.D., Ed., Plenum Press, New York, NY, 1985 Vol. 2 pp 35.
69. Carr P.W. Li J. Dallas A.J. Eikens D.I. and Tan L.C. *J. Chromatog. A.* 1993, 656, 113-133.
70. Noll, K.E. and Gounaris, V., *Adsorption Technology for Air and Water Pollutant Control*, Lewis Chelsea, MI USA, 1991.
71. Smith, M.S. *Chemical Engineering Kinetics*, 3<sup>rd</sup> edn., McGraw-Hill New York NY, USA, 1981
72. Adamson, A.W. *Physical Chemistry of Surfaces*, 5<sup>th</sup> edn., Willey, New York NY, USA, 1990
73. Gregg, S.J. and Sing K.S.W. *Adsorption, Surface Area and Porosity*, 2<sup>nd</sup> edn., Academic Press, New York NY, USA, 1982
74. Stanley B.J. and Guiochon G. *Langmuir*, 1995, 11 1735-1743
75. Graham, D. *J. Phys. Chem.*, 57, 1953, 665
76. Laub, R.J. *ACS Symp. Ser.*, 297, 1986, 1
77. Toth J. *Acta Chim. Acad Sci. Hung.*, 1971 69, 311
78. Quinones I., Ford J.C. and Guiochon G. *Chem. Eng. Sci.* 2000,55, 909-929
79. Hasen H.K., Sasmussen P., Fredenslund A., Schiller M. and Gmehling J., *Ind. Eng. Chem. (Res)*, 30, 1991, 2352-2355
80. Sadroddin Golshan-Shirazi, Jun-Xiong Huang, I and Georges A. Guiochon *AMI. Chm.* 1991, 63, 1147-1154

81. Glueckauf, E. *J. Chem. Soc.*, 1947, 1302
82. Conder, J.R. and Young C.L. *Physicochemical Measurement by Gas Chromatography*. Wiley, New York, 1979 pp 353-429
83. James, D.H. and Phillips, C.S.G. *J. Chem. Soc.* 1954 1066
84. Schay, G. and Szekely G., *Acta. Chim. Hung*, 5,1954, 167
85. Cremer, E. and Huber J.F.K. *Angew. Chem.* 73, 1961, 461
86. Reilley, C.N.; Hidebrand G.P and Ashley Jr. J.W. *Anal. Chem.* 34,1962, 1198
87. Rodriguez, J.B. and Lendl B. Andrew E., Diewok J. *Anal. Bioanal. Chem.* 376, 2003, 92-97
88. Katinonkul, W. MS thesis, IUP, Indiana, PA, 2003
89. Ashcroft, N. W. and Mermin, N. D. *Solid State Physics* (Harcourt: New York, 1976)
90. Chan, C. D. N.  
[http://en.wikipedia.org/wiki/Image:indices\\_miller\\_direction\\_examples.png](http://en.wikipedia.org/wiki/Image:indices_miller_direction_examples.png)
91. Chan, C. D. N.  
[http://en.wikipedia.org/wiki/Image:indices\\_miller\\_plan\\_definition.png](http://en.wikipedia.org/wiki/Image:indices_miller_plan_definition.png)
92. Nix, R. M. [http://www.chem.gmul.ac.uk/surfaces/chem/scc/scat1\\_2.htm](http://www.chem.gmul.ac.uk/surfaces/chem/scc/scat1_2.htm), 2002
93. [http://mrsec.wisc.edu/Edetc/course/chem\\_801\\_ProbSet\\_Answerkey.pdf](http://mrsec.wisc.edu/Edetc/course/chem_801_ProbSet_Answerkey.pdf)
94. Macrae, R. M. <http://www.fhi-berlin.mpg.de/th/personal/hermann/fccnet.gif>
95. Haymond S., Babcock G.T., Swain G.M. *J. Am. Chem. Soc.* 124, 2002, 10634-10635
96. Pate B.B. *Surf. Sci.* 165, 1986, 83,
97. Scholze A.; Schmidt W.G.; Bechstedt R. *Phys. Rev. B* 53(20), 1995, 13725-13733
98. Hamsher, A. *BS Research*, IUP, Indiana, PA 2006
99. Bobrov K.; Comtet G.; Hellner L; Dujardin G. *Applied Physical Letters* 85(2), 2004, 296-298
100. Talbot-Ponsonby D.F.; Newton M.E.; Baker J.M.; Scarsbrook G.A.; Sussmann

- R.S.; Whitehead A.J.; Pfenninger S. *Phys.Rev. B.* 57, 1998, 2264
101. Poprici G.; Wilson R.g.; Sung T.; Prelas M.A.; Khasawina S. *J. App. Phys.* 70, 1995, 5103
  102. Barnard A.S.; Sternberg M. *J. Phys. Chem. B.* 109, 2005, 17107-17112
  103. Giddings, J. C. *Unified Separation Science*, John Wiley and Sons INC., NY, 1991
  104. Rimmer C., A., Simons C., R., Dorsey J., *J. Chromatogr. A* 965 (1/2), 2002, 219.
  105. Knox, J.H., Kaliszan, R., *J. Chromatogr.* 349,1985, 211.
  106. Leonard M. *J. Chromatogr B*, 699, 1997, 3-27
  107. Yao Y., Lenhoff A. M., *J. Chromatogr A*, 1126, 2006, 107–119
  108. Schure M., R., and Maeir R., S., *J. Chromatogr. A.* 126 (1/2), 2006, 58,.
  109. Hemetsberger, H., Maasfeld, W. , Ricken, H. *Chromatographia*, 9(7), 1976, 303-310
  110. Frank H.S., Evans M.W., *J. Chem. Phys.* 13 (11), 1975, 507
  111. Afzal M., Mahmood f., AND Saleen M., *Colloid and Polymer Science.* 270 (9), 1992, 917
  112. Grifitts G.D., Marshall, K., Rochester C.H., *J. Chem. Soc.. Faraday Trans.* 1(70), 1974, 400
  113. Okunev A.G., Paukshtis E.A., Aristov Y. I. *React. Kinet.. Catal. Lett.* 65 (1) 1998, 161
  114. Parfitt G.D., Rochester C.H., *Adsorption from solution at the Solid/Liquid Interface.* Academic Press, NY 1983
  115. Van Danne H., Levitz P., Bergaya F., Alcover J.F., Gatineau L., Fripiat J.J., *J. Chen. Phys.* 85, 1986, 616